

Automatic Geometric Decomposition for Analytical Inverse Kinematics

Daniel Ostermeier, Jonathan Külz, and Matthias Althoff

Abstract—Calculating the inverse kinematics (IK) is a fundamental challenge in robotics. Compared to numerical or learning-based approaches, analytical IK provides higher efficiency and accuracy. However, existing analytical approaches are difficult to use in most applications, as they require human ingenuity in the derivation process, are numerically unstable, or rely on time-consuming symbolic manipulation. In contrast, we propose a method that, for the first time, enables an analytical IK derivation and computation in less than a millisecond in total. Our work is based on an automatic online decomposition of the IK into pre-solved, numerically stable subproblems via a kinematic classification of the respective manipulator. In numerical experiments, we demonstrate that our approach is orders of magnitude faster in deriving the IK than existing tools that employ symbolic manipulation. Following this one-time derivation, our method matches and often surpasses baselines, such as IKFast, in terms of speed and accuracy during the computation of explicit IK solutions. Finally, we provide an open-source C++ toolbox with Python wrappers that substantially reduces the entry barrier to using analytical IK in applications like rapid prototyping and kinematic robot design.

Index Terms—Kinematics, Computational Geometry, Software Tools for Robot Programming.

I. INTRODUCTION

INVERSE kinematics (IK) describes the problem of finding joint angles of a kinematic chain for a given end-effector pose. The IK problem is known to be analytically solvable for a specific set of kinematic chains that fulfill certain geometric properties [1]. Industrial robots are often designed with these properties in mind. In these cases, human-driven manual derivation of an analytical IK is time-consuming but feasible, as it is only done once during the entire engineering process. Recently, computational design methods for monolithic [2], [3] or modular robots [4], [5] have proven promising in optimizing industrial robots. They are based on iterative optimization and feature many kinematically distinct manipulators in dynamic problem settings. Manually deriving an analytical IK for each possible manipulator design is time-consuming, requires domain expertise, and, hence, is usually

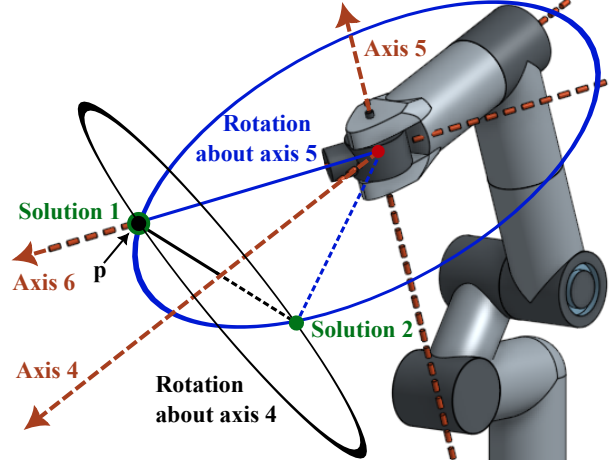


Fig. 1. When solving the IK for a 6-DOF robot with a spherical wrist, we obtain the angles for its axes four and five via the visualized subproblem. A unit circle is hereby centered around axes four (black) and five (blue). Each unit circle is contained in a plane whose normal vector aligns with the respective axis. Both planes contain the point p : A unit offset originating from the intersection point of the last three axes (red dot) along axis six. The intersection points of the two unit circles resemble the potential solutions to this subproblem. The solutions to all other angles are obtained in a similar fashion. Invalid solutions, i.e., Solution 2, are discarded in the process.

infeasible. Existing methods that automatically derive the analytical IK either rely on symbolic manipulation—which takes several minutes per manipulator—or are numerically unstable in the vicinity of singularities and workspace boundaries. Due to these limitations of existing analytical solvers, less accurate, computationally intensive numerical methods that yield incomplete solutions are a typical choice in the mentioned applications, even if analytical solutions are known to exist. Our work represents the first approach to enable analytical IK in real-time computational manipulator design, e.g., for modular robots. The proposed method is based on geometric feature matching against a set of known kinematic classes. Through this classification process, we rapidly identify analytically solvable kinematic chains. The IK problem of these chains is decomposed into a series of geometric subproblems. Both the kinematic classification (conducted once per manipulator) and the subsequent evaluation of the subproblems (conducted once per desired end-effector pose) are real-time-capable and do not require human intervention or symbolic manipulation. We further propose an automated kinematic remodeling procedure that makes our method applicable to arbitrary parameterizations of the kinematic chain, such as a Unified Robot Description Format (URDF) file, Denavit-Hartenberg (DH) parameters [6], or homogeneous coordinates

Received 7 May 2025; accepted 18 July 2025, 2025; Date of publication 11 August 2025. This article was recommended for publication by Associate Editor L. Scalera and Editor L. Pallottino upon evaluation of the Associate Editor and Reviewers' comments. This work was supported by the Deutsche Forschungsgemeinschaft (German Research Foundation) under grant number AL 1185/31-1. (Corresponding Author: Daniel Ostermeier)

Daniel Ostermeier is with the Department of Computer Engineering, Technical University of Munich, 85748 Garching, Germany (e-mail: daniel.sebastian.ostermeier@tum.de).

Jonathan Külz and Matthias Althoff are with the Department of Computer Engineering, Technical University of Munich, 85748 Garching, Germany, and also with the Munich Center for Machine Learning (MCML), 80333 Munich, Germany (e-mail: jonathan.kuelz@tum.de; althoff@tum.de).

Digital Object Identifier (DOI): 10.1109/LRA.2025.3597897

TABLE I
COMPARISON OF PREDOMINANT METHODS FOR ANALYTICAL IK.

	Ours	IKFast [8]	Eigenstructure [9], [10]	Elias et al. [7]
Automatic derivation	Yes	Yes	Yes	No
Numerically stable	Yes	Yes	*	Yes
Code available	Yes	Yes	No	Yes
Classes Fig. 2	3, 5–9	2–9**	2–9**	8, 9

*Numerical stability is doubted [8], [11].

**The actual limits of these methods are insufficiently known.

of the joint frames in the zero configuration. Our method is currently limited to non-redundant manipulators with revolute joints. For redundant manipulators (e.g., $\geq 7R$), our method can be used to search for a set of joints that, when locked in place, allow us to analytically solve the resulting kinematics. To solve the subproblems that we obtain from our decomposition algorithm, we leverage the numerically stable solutions introduced by Elias et al. [7], which we extend to an even larger share of kinematic classes than initially considered. We implement our method in our open-source toolbox Efficient Analytical Inverse Kinematics (EAIK). Additional visualizations and an introduction guide are available on our project website: <https://eaiik.cps.cit.tum.de>.

II. RELATED WORK

Most approaches for solving the IK problem can be split into analytical, numerical, and learning-based methods. Numerical methods involve iterative algorithms that gradually refine an initial guess for the joint configuration until a desired end-effector pose is achieved. To this end, many approaches use the inverse or pseudo-inverse of the manipulator Jacobian [12, Chapter 6.2]. Alternatively, the IK can be described as a high-dimensional minimization problem, so arbitrary numerical optimization algorithms can be deployed, optionally, under consideration of additional constraints [13]. Compared to analytical approaches, numerical IK has an increased computation time, can suffer from numerical instability, and usually only provides a single solution [14]. Learning-based methods, such as IKFlow [15], can be advantageous for redundant manipulators [16] by drawing diverse samples from infinite solution spaces. However, these methods do not generalize well across different manipulators, which renders them useless if the manipulator topology is not known a priori.

While a general solution for analytical IK is yet to be discovered, a wide range of works [17]–[19] focuses on hand-derived IK formulations for specific manipulators. Fundamental aspects of a more broadly applicable method date back to the 1960s, when Donald L. Pieper [1] proposed a polynomial-based approach alongside two sufficient conditions—nowadays known as “Pieper criteria”—for the existence of an analytical solution: Assuming a non-degenerate robot, he states that any 6R manipulator is solvable given that either (a) the last or first three joint axes of a manipulator intersect in a common point (as shown in Fig. 1) or (b) three consecutive intermediate joint axes of the robot are parallel.

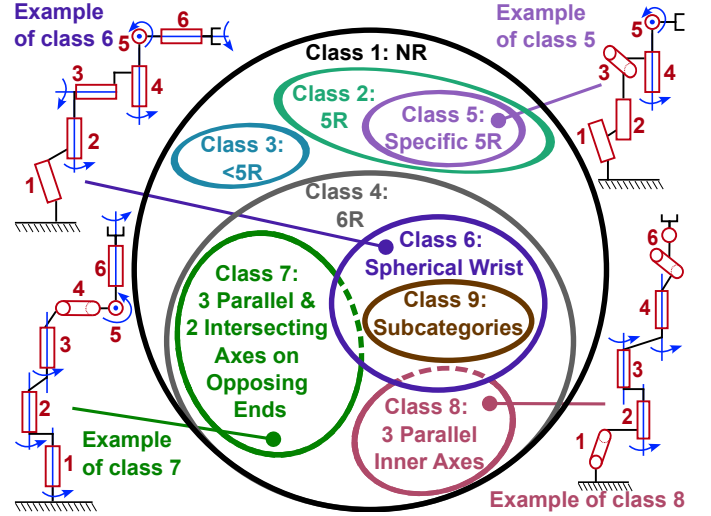


Fig. 2. We assign classes to certain sets of kinematic chains. All depicted classes except 1, 2, and 4 are solvable by our method. The subproblem decompositions for classes 8 and 9 have already been derived in [7]. Further distinctions within the classes are necessary for the decompositions in the Appendix, but are not depicted for simplicity.

Furthermore, all non-degenerate 3R manipulators are known to be analytically solvable [20]. The only widely acknowledged necessary condition for the existence of an analytical IK is for the manipulator chain to be non-degenerate [11]. Degeneracy occurs if the last link of a kinematic chain has fewer degrees of freedom than the kinematic chain has joints—either for specific end-effector poses (singularities) or for all possible poses within its workspace (implicit redundancies) [1]. While manipulators with seven or more degrees of freedom are inherently degenerate, solutions can be derived by joint-locking [21]–[23] or a fixed (arm) angle in the case of elbow manipulators [18], [24]–[26]. For non-degenerate manipulators, [27] proposes an approach based on conformal geometric algebra to solve the IK for robots with spherical wrists. A similar framework is proposed in [28], where a semi-analytical method for manipulators with arbitrary rotational joints is developed.

A common approach for deriving IK solutions is decomposing the problem into geometric subproblems [29], [30]. Subproblems define a distinct set of geometric correspondences for which the analytical solution is known a priori. One seeks to re-obtain these subproblems as decoupled, individually solvable terms in the IK formulation of a manipulator by exploiting collinearities and intersections between certain joint axes. Previous work proposes different subproblem representations [31], [32]. Further canonical sets of pre-solved subproblems are presented in [7], [29], [30], [33]. In this work, we build directly on the canonical set proposed by Elias et al. [7]. While they derive the IK formulations for certain 6R manipulators, their derivations depend on coinciding reference points for intersecting joint axes, which often require tedious manual reformulations of the manipulator kinematics. Furthermore, the authors do not elaborate on how a feasible decomposition can be automatically chosen for a given manipulator.

Approaches on general solvers, such as IKFast [8], aim to

automate the analytical IK derivations. IKFast relies on symbolic manipulation of the IK equations and tangent-half-angle substitution to derive respective univariate polynomials as proposed by Raghavan and Roth [34] and, e.g., adopted in [35]. In [36], the approach of Raghavan and Roth is compared to a subproblem-based IK formulation, where the latter showed higher accuracy, robustness, and computational efficiency. The IK problem may also be defined as an eigenstructure problem, as shown by [9], [10]. The numerical stability of these eigenstructure-based approaches, however, is doubted in more recent publications [8], [11]. Another take on general symbolic solvers is presented in [11], where behavior trees are used to break up the symbolic IK formulations following a rule-based approach. In [37], the authors propose an algorithm similar to the subproblem decompositions presented in our work, but with the sole motivation of deciding on analytical solvability.

Prior work on manipulator design focuses on kinematic properties such as static reachability [4], [5], [38]–[41], dexterity [42], or coverage of a pre-defined workspace [43], [44]. Efficiently evaluating these properties requires solving the IK for many novel manipulator designs. While analytical solvers are theoretically applicable in this context, all existing general solvers exhibit one of two limitations in this context: either the derivation process, e.g., generating a C++ file, takes multiple minutes, or the resulting solver is considered unstable in the vicinity of workspace boundaries or singularities. Our work addresses these limitations by combining fast derivations with stable solutions for a broad class of manipulators.

III. NOTATION AND PROBLEM STATEMENT

A. Notation

This work is limited to kinematic chains of rigid bodies connected by revolute joints. To represent the kinematics, we employ an exponential coordinate representation for rotations [12, Chapter 3.2.3], paired with three-dimensional Cartesian displacement vectors that represent the position offset between two joint axes.

Let \mathbb{S}^1 represent the unit circle in the plane and for $n \in \mathbb{N}_+$: $\mathbb{Q} = \mathbb{S}_1^1 \times \dots \times \mathbb{S}_{n-1}^1$ [45, Chapter 3.2.1]. The kinematics of a manipulator with n revolute joints and joint space \mathbb{Q} are fully defined by n joint axes with respect to a basis frame Σ_0 , and the static orientation of the end effector relative to the last joint axis. Each joint axis is specified by a unit vector $\mathbf{h}_j \in \mathbb{R}^3$ that is expressed in the basis frame, and a reference point ${}^0\mathbf{p}_j \in \mathbb{R}^3$ on the axis. We write ${}^j\mathbf{p}_k$ to denote the translational offset between the reference points of axes j and k . $\mathbf{R}(\mathbf{h}_j, \theta_j) \in \text{SO}(3)$ denotes the rotation matrix that corresponds to a rotation about the unit vector \mathbf{h}_j by angle θ_j . We omit the argument for readability and write ${}^{j-1}\mathbf{R}_j$ for the remainder of this paper to denote the rotation induced by rotating the j -th joint. We generalize this notation to ${}^i\mathbf{R}_k$, where $i < k - 1$, to represent consecutive rotations about $\mathbf{h}_{i+1}, \dots, \mathbf{h}_k$ by the corresponding joint angles. Further, ${}^0\mathbf{R}_{EE} = {}^0\mathbf{R}_j {}^j\mathbf{R}_{EE}$ represents the rotation between the base frame and the end-effector frame given the static rotation ${}^j\mathbf{R}_{EE}$.

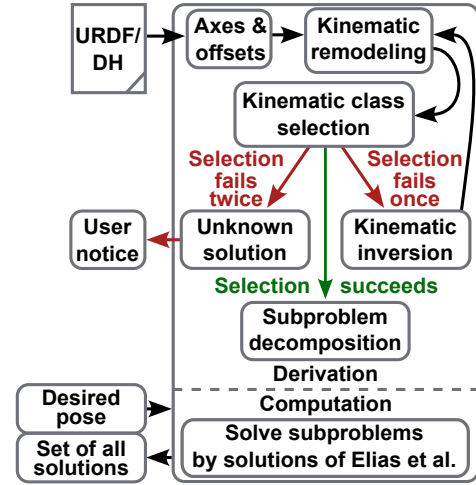


Fig. 3. Flow diagram: Assigning a manipulator to a kinematic class.

B. Problem statement

The forward kinematics (FK) function $\text{FK} : \mathbb{Q} \rightarrow \text{SE}(3)$ of the manipulator returns the end-effector pose $\mathbf{T}_{EE} \in \text{SE}(3)$ for the joint angles $\boldsymbol{\theta} \in \mathbb{Q}$ and can be computed in various ways, e.g., using the product of exponentials formula or the equation of Rodrigues [12, Chapter 4]. We define the position FK according to (1) and the orientation FK via (2).

$${}^0\mathbf{p}_{EE} = {}^0\mathbf{p}_1 + \left(\sum_{i=1}^{n-1} {}^0\mathbf{R}_i {}^i\mathbf{p}_{i+1} \right) + {}^0\mathbf{R}_n {}^n\mathbf{p}_{EE} \quad (1)$$

$${}^0\mathbf{R}_{EE} = \left(\prod_{i=0}^{n-1} {}^i\mathbf{R}_{i+1} \right) {}^n\mathbf{R}_{EE} \quad (2)$$

Given a desired pose \mathbf{T}_D , we want to find the discrete set of all analytically feasible solutions to the IK problem

$$\text{IK}(\mathbf{T}_D) = \{ \boldsymbol{\theta} \in \mathbb{Q} \mid \text{FK}(\boldsymbol{\theta}) = \mathbf{T}_D \}. \quad (3)$$

We do not impose any order on the obtained solutions.

IV. METHOD

We assume that the kinematic structure of a manipulator follows the convention in Section III-A, which can be easily obtained from a URDF¹ file, DH parameters [6], or likewise. Prior works [7], [31], [32] showed that the IK problem for specific manipulators is solvable by decomposing its kinematic formulation into analytically solvable subproblems by hand. To automate this process, we start by *remodeling* the given kinematic chain. We thereby shift the reference points on the joint axes such that the following properties realize a simplification of $\text{IK}(\mathbf{T}_D)$:

- According to (1), the position kinematics of a manipulator is invariant to a rotation ${}^0\mathbf{R}_j$ whenever ${}^j\mathbf{p}_{j+1} = \mathbf{0}$.
- If two or more joint axes are parallel or anti-parallel, their unit vectors \mathbf{h}_i can be chosen equally by negating the rotation angle, and consecutive rotations can be grouped in a single rotation according to the rotation formula of Rodrigues [12, Chapter 4].

¹Elaboration on the URDF: <https://wiki.ros.org/urdf>

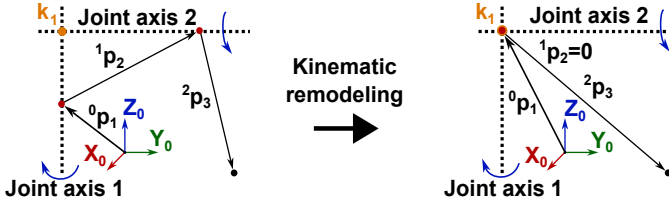


Fig. 4. Kinematic remodeling for the example of two intersecting axes: We translate the reference points (red dots) along the corresponding axes until they coincide. Black dots mark reference points of the subsequent axes.

After remodeling, we assign each manipulator to a kinematic class (see Fig. 2).

An overview of our proposed method is shown in Fig. 3. Subproblem decompositions for classes 8 and 9 are given by [7]. Additionally, we obtain decompositions for class 3 and classes 5–7 using the derivations presented in the Appendix and on our website. If a subproblem decomposition is not known for the resulting class, we invert the chain as described in Section IV-C and try again. If the remodeling and inversion procedure yields a class with a known decomposition, we can obtain the complete analytical solution set for arbitrary end-effector poses in the workspace. We refer to remodeling, inversion, and class assignment as the derivation process.

To cope with analytically unsolvable manipulators (e.g., with seven or more joints), we can employ an *uninformed search* for a set of joints that, when locked in place, yields a solvable manipulator. This is done by iterating over all possible combinations of locked joints and applying the derivation algorithm in Fig. 3. Up until now, to the best of our knowledge, such a search algorithm could not be employed with mathematical certainty (i.e., via analytical expressions) in a reasonable time and is only made feasible by the fast derivation times of our method.

A. Kinematic remodeling

The detection of parallel and anti-parallel axes is straightforward. Translational offsets between the reference points on the joint axes, on the other hand, are typically non-zero for common parametrizations of real-world manipulators. We obtain a zero-valued offset for two or more consecutive intersecting axes by moving their corresponding reference points to the point where the axes intersect, as visualized in Fig. 4. We compute the intersection point of two axes by following the approach from [46]. If two axes do not intersect perfectly, e.g., due to numerical inaccuracies, it yields the closest point to both axes.

We denote the intersection point of two joint axes j and $j+1$ as $\mathbf{k}_j \in \mathbb{R}^3$. As \mathbf{k}_j is located on both joint axes j and $j+1$, we can shift their reference points ${}^0\mathbf{p}_j$ and ${}^0\mathbf{p}_{j+1}$ to coincide with \mathbf{k}_j . As a result, ${}^j\mathbf{p}_{j+1} = \mathbf{0}$. Both ${}^{j-1}\mathbf{R}_j$ and ${}^j\mathbf{R}_{j+1}$ are hereby left unchanged, and so is (2). However, we need to further assure that (1) is invariant to our remodeling. We hence adjust the preceding and subsequent displacement

vectors:

$${}^{j-1}\mathbf{p}_j = \mathbf{k}_j - {}^0\mathbf{p}_{j-1} \quad (4)$$

$${}^j\mathbf{p}_{j+1} = \mathbf{0} \quad (5)$$

$${}^{j+1}\mathbf{p}_{j+2} = {}^0\mathbf{p}_{j+2} - \mathbf{k}_j. \quad (6)$$

If the first two joint axes intersect ($j = 0$), we can omit the adjustment in (4) by choosing our base frame such that its origin coincides with the first reference point. This procedure is not always unique, as an axis can intersect with both the preceding and succeeding axes in the kinematic chain, but at different intersection points. In this case, we choose the first representation to which we can apply a known decomposition.

B. Subproblem decompositions

Singular configurations of the robot, or end-effector poses in the proximity of workspace boundaries, often pose an issue to analytical methods due to numerical instabilities. We employ the subproblems introduced in [7], which are posed such that approximate least-squares² solutions are obtained if no finite set of exact solutions exists. Continuous and stable IK solutions are thereby guaranteed even when facing singularities. The authors in [7] further derive subproblem decompositions for predominant 6R manipulator families, and hint at some additional cases for manipulators containing specific intersecting or parallel axes. We adapt their derivations in our method and complement their work by providing explicit solutions to the missing cases in the Appendix.

Non-degenerate 1R, 2R, 3R, and 4R manipulators (class 3) are solvable even without additional intersecting or parallel axes. On the other hand, 5R manipulators are solvable per our method if contained in class 5, i.e., if they meet at least one of the following sufficient criteria:

- The last or first two axes 1,2 (5,6) intersect.
- The intermediate axes 2,3 (3,4) intersect while the axes 3,4 (2,3) are parallel.
- Any three consecutive axes are parallel.

The derivations for all manipulators with fewer than six joints follow the same scheme we applied in the Appendix. For brevity, we refrain from explicitly denoting the obtained decompositions and their derivations here, but instead present them on our project website in a separate document: <https://eaik.cps.cit.tum.de>.

C. Kinematic inversion

We extend the introduced derivations to an even broader set of manipulators, i.e., those that are created by switching end effector and basis of the derived manipulators, by inverting their kinematic chain. Hereby, we redefine:

$$\mathbf{h}'_j = -\mathbf{h}_{n-j+1}, \quad j \in \{1, \dots, n\} \quad (7)$$

$${}^j\mathbf{p}'_{j+1} = -{}^{n-j}\mathbf{p}_{n-j+1}, \quad j \in \{1, \dots, n\}. \quad (8)$$

²These least-squares formulations minimize the error of each subproblem. The solutions may not correspond to the global least-squares formulation for the Euclidean distance between the end effector and desired pose.

Hence, we obtain new position and orientation forward kinematics for the redefined joint axes with

$${}^0\mathbf{p}'_n = \sum_{k=n}^1 {}^k\mathbf{R}_{k-1} {}^k\mathbf{p}_{k-1} = -{}^0\mathbf{R}_n^T {}^0\mathbf{p}_n \quad (9)$$

$${}^0\mathbf{R}'_n = \prod_{k=n}^1 {}^k\mathbf{R}_{k-1} = {}^0\mathbf{R}_n^T. \quad (10)$$

The joint angles are invariant with respect to the inversion procedure. Hence, we can compute any IK problem of the original (non-inverted) kinematic chain by solving the IK of its inverted chain for the inverse of the original end-effector pose.

V. EXPERIMENTAL EVALUATION AND COMPARISON

We compare our method to different frameworks on common 6R manipulators: the UR5 robot (three parallel and two intersecting axes, [class 8](#)), the Puma (spherical wrist and two intersecting axes, [class 9](#)), and the ABB IRB 6640 (spherical wrist and two parallel axes, [class 9](#)). A Franka Emika Panda (spherical wrist after kinematic inversion, [class 6](#)) represents the category of redundant 7R robots, which we solve by locking joint 7. We further use two fictitious manipulators from [7]: The “Spherical” (spherical wrist, [class 9](#)) and “3-Parallel” (three parallel axes, [class 8](#)) robot. Although derivations for these manipulators were already shown in [7], the URDF and DH parameterizations used in our experiments did not naturally exhibit coinciding joint frames at axis intersection points. Hence, the original derivations fail when applied directly and rely on a tedious reformulation of the manipulator kinematics by a human. Our method resolves this issue via kinematic remodeling and inversion. We compare the computation speed and accuracy of our method to that of IKFast [8], the learning-based IKFlow method [15], as well as the numerical Gauss-Newton (GN) and Levenberg-Marquardt (LM) solvers implemented in the Python Robotics Toolbox [47]. Our experiments with IKBT [11] showed certain problems ranging from slow file generation to non-functional code. In our opinion, its strength lies in the fully symbolic output in the form of LaTeX code. Other publicly available solvers, like YAIK³, show promising results but lack an underlying scientific publication and basic documentation. As IKFast is well-maintained and the current standard way of deriving analytical IK, it serves as the baseline against which we compare. All experiments were conducted on an AMD Ryzen 7 8-core CPU.

A. Computational efficiency

Table II shows the initial derivation time to obtain an analytical IK solution for our approach and IKFast. For our method, we also distinguish between an optimized DH parametrization with direct access to the underlying C++ implementation and a URDF-based parametrization that includes larger parts of unoptimized Python code to obtain the representation we define in Section III-A. The latter allows for a fairer comparison

to IKFast, which depends on a similar file format. In the case of IKFast, the derivation time includes the duration of code generation without compilation. For our method, the measured time includes a single run of the forward kinematics calculation to obtain the positions of all joint axes in zero-pose, the remodeling of the kinematic chain, and the kinematic class selection. The results clearly show the main advantage of our method (EAIK) over existing tools: The automatic remodeling and decomposition into subproblems is orders of magnitude faster than the automatic code generation of IKFast. In the specific example of the UR5 robot, IKFast takes more than 15 minutes compared to 39 μ s using EAIK. The mean derivation time of our method was below 50 μ s for all evaluated 6R robots.

After derivation, we generate 5,000 IK problems for each robot by calculating the forward kinematics for randomly sampled joint angles. Fig. 5a shows the computation times for IKFast, both numerical approaches, and EAIK. We also compare the methods with respect to the 7R Franka Panda manipulator and include timings for its hand-derived analytical IK by He et al. [48]. All of the analytical methods rely on joint locking for the Panda, so we set the last joint to a fixed random value. Except for the Puma, the Panda, and some rare outliers, where IKFast performs extraordinarily well, our implementation manages to surpass the computation speed of IKFast by a factor of at least five. The measured times correspond to a single solution for the numerical approaches and the set of all possible solutions for EAIK, IKFast, and He et al., respectively. As expected, both numerical solvers are significantly slower than EAIK and IKFast. The highly specialized method by He et al. serves as a baseline for how fast manual implementations are when tailored to a specific manipulator. It performs best for the Panda but inherently fails when applied to one of the other presented manipulators.

Additionally, we evaluate a scenario inspired by modular robot design, where IK solutions are required for a large variety of different manipulators [4], [5], [39]. We generate a batch of 10,000 6R manipulators (belonging to analytically solvable kinematic classes) via randomized DH parameters and sample one random pose from the workspace of each manipulator. Prior to our work, long derivation times disqualified most analytical methods from being used in such challenging tasks, with numerical methods remaining the only option—even if analytically solvable robots, as in [39], make up the major part of the design space. The combined time for IK derivation and computation is displayed in Fig. 5b, which shows that our method is consistently faster than both numerical methods, all while computing the full solution set.

To compare our approach to the learning-based IKFlow, we again choose the 7R Panda robot. While comparison on a 6R robot would be more representative, the authors do not provide pre-trained networks for such manipulators. Our own endeavors in training their network to the UR5 resulted in position errors in the order of multiple centimeters, which we deem not representative. To solve the Panda analytically, we lock joint seven in a random position. IKFlow is able to make use of all seven joints. Our experiments show a mean computation time of 75.07 μ s for IKFlow (7507 μ s per batch

³YAIK implementation: <https://github.com/weigao95/yaiik>

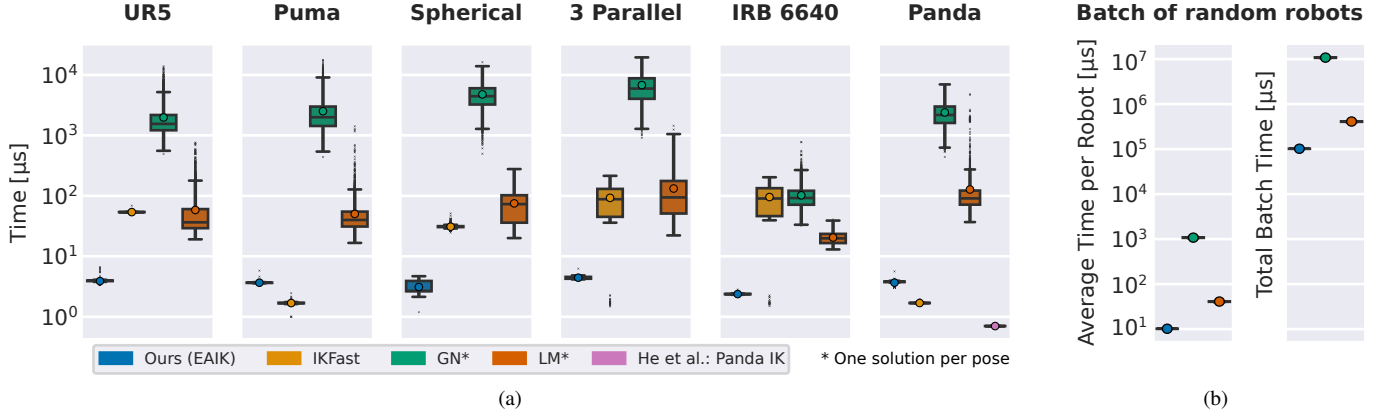


Fig. 5. Comparison of the IK computation times of five representative manipulators on 5,000 randomly assigned end-effector poses (a) and the batch-times on 10,000 random (analytically solvable) 6R manipulators (b). The measured times in (a) correspond to a single solution for the numerical approaches—which we marked with an asterisk—and the set of all possible solutions for EAIK, IKFast, and the method by He et al. [48], respectively. In (b), we include derivation times and only show our method along with the numerical ones, as the derivation times of IKFast are too long for this task to finish within a reasonable time. Our method shows the smallest overall variance and, except for the Puma and Panda robot, consistently surpasses all other methods.

TABLE II
DERIVATION TIMES FOR ANALYTICAL IK SOLUTIONS.

	Ours (URDF)	Ours (DH)	IKFast
IRB6640	36 μ s	3.7μs	22 \cdot 10 ⁶ μ s
Spherical	36 μ s	3.9μs	16 \cdot 10 ⁶ μ s
UR5	39 μ s	3.6μs	95 \cdot 10 ⁷ μ s
Puma	35 μ s	3.8μs	37 \cdot 10 ⁶ μ s
3-Parallel	36 μ s	3.3μs	53 \cdot 10 ⁷ μ s
Panda (Joint 7 locked)	45 μ s	6.3μs	93 \cdot 10 ⁶ μ s

of 100 poses) and 3.67 μ s for our method. IKFlow is only able to perform batched computations.

B. Accuracy

The accuracy of analytical methods (i.e., ours and IKFast) is only limited by the chosen floating-point representation and the numeric errors that originate from mathematical operations within it. The solutions we obtain via IKFlow for the Panda manipulator result in a median position error of 7.3×10^{-3} m. The median position error of our approach is 1.12×10^{-15} m using the same poses as with IKFlow on the Panda. The error of our method thereby lies within the expected double-precision floating-point accuracy. When evaluated on the UR5 robot, the numerical methods (GN and LM) show a similar median position error of about 10^{-4} m. This is multiple orders of magnitude higher than the median error of our method (10^{-15} m) and IKFast (10^{-12} m) for the same experimental setup. The error on the numerical solvers vastly depends on the number of iterations undergone (up to 30 in our case) and poses a trade-off between accuracy and computation time. A quantitative comparison of different numerical solvers and their respective parameters is available in [14], [49].

VI. CONCLUSION

Our approach for solving IK problems based on subproblem decomposition is automatic, real-time capable, and numerically stable. Current analytical solvers either require manual

derivations at some point, rely on slow symbolic manipulation, or are numerically unstable. Our open-source implementation substantially lowers the entry barrier for using analytical IK. It facilitates the use of analytical IK in domains where the properties of a kinematic chain change frequently, such as in (modular) robot design, where derivation times of multiple seconds or even minutes rendered analytical approaches unfeasible in the past.

While we present an extensive set of analytically solvable kinematic classes, there may exist more sufficient conditions that allow us to decompose novel kinematic classes to obtain analytical solutions. Our method is currently incapable of solving parallel kinematic chains, manipulators with joints that are not revolute, or robotic systems with multiple end effectors. Further, joint limits, trajectory consistency, and collision constraints need to be verified a posteriori by computing the full-body forward kinematics for the identified solutions. Possible future work includes: (a) the integration of (semi-)numerical fallbacks for manipulators with no known subproblem decompositions, e.g., via the search-based approach in [7], (b) explicit parametrizations for detected internal redundancies, and (c) solutions for manipulators with linear axes or parallel joint configurations.

REFERENCES

- [1] D. L. Pieper, “The kinematics of manipulators under computer control,” Ph.D. dissertation, Department of Mechanical Engineering, Stanford University, 1968.
- [2] M. Sorokin, *et al.*, “On designing a learning robot: Improving morphology for enhanced task performance and learning,” in *Proc. of the IEEE/RSJ Int. Conf. on Intelligent Robots and Systems (IROS)*, 2023, pp. 487–494.
- [3] A. Vaish and O. Brock, “Co-designing manipulation systems using task-relevant constraints,” in *Proc. of the IEEE Int. Conf. on Robotics and Automation (ICRA)*, 2024, pp. 4177–4183.
- [4] J. Whitman, *et al.*, “Modular robot design synthesis with deep reinforcement learning,” in *Proc. of the AAAI Conf. on Artificial Intelligence (AAAI)*, vol. 34, no. 06, 2020, pp. 10 418–10 425.
- [5] J. Külz and M. Althoff, “Optimizing modular robot composition: A lexicographic genetic algorithm approach,” in *Proc. of the IEEE Int. Conf. on Robotics and Automation (ICRA)*, 2024, pp. 16 752–16 758.

- [6] J. Denavit and R. S. Hartenberg, "A kinematic notation for lower-pair mechanisms based on matrices," *Applied Mechanics*, vol. 22, no. 2, pp. 215–221, 1955.
- [7] A. J. Elias and J. T. Wen, "IK-Geo: Unified robot inverse kinematics using subproblem decomposition," *Mechanism and Machine Theory*, vol. 209, no. 105971, 2025.
- [8] R. Diankov, "Automated construction of robotic manipulation programs," Ph.D. dissertation, Robotics Institute, Carnegie Mellon University, 2010.
- [9] D. Manocha and Y. Zhu, "A fast algorithm and system for the inverse kinematics of general serial manipulators," in *Proc. of the IEEE Int. Conf. on Robotics and Automation (ICRA)*, vol. 4, 1994, pp. 3348–3353.
- [10] D. Manocha and J. Canny, "Efficient inverse kinematics for general 6R manipulators," *Transactions on Robotics and Automation*, vol. 10, no. 5, pp. 648–657, 1994.
- [11] D. Zhang and B. Hannaford, "IKBT: Solving symbolic inverse kinematics with behavior tree," *Artificial Intelligence Research*, vol. 65, pp. 457–486, 2019.
- [12] K. M. Lynch and F. C. Park, *Modern Robotics: Mechanics, Planning, and Control*, 1st ed. Cambridge University Press, 2017.
- [13] A. Aristidou and J. Lasenby, "Fabrik: A fast, iterative solver for the inverse kinematics problem," *Graphical Models*, vol. 73, no. 5, pp. 243–260, 2011.
- [14] J. Haviland and P. Corke, "Manipulator differential kinematics: Part 1: Kinematics, velocity, and applications," *Robotics & Automation Magazine*, pp. 2–11, 2023.
- [15] B. Ames, J. Morgan, and G. Konidaris, "IKFlow: Generating diverse inverse kinematics solutions," *IEEE Robotics and Automation Letters*, vol. 7, no. 3, 2022.
- [16] R. Bensadoun, *et al.*, "Neural inverse kinematics," in *Proc. of the Int. Conf. on Machine Learning (ICML)*, vol. 162, 2022, pp. 1787–1797.
- [17] T. Ho, C.-G. Kang, and S. Lee, "Efficient closed-form solution of inverse kinematics for a specific six-DOF arm," *Control, Automation and Systems*, vol. 10, no. 3, pp. 567–573, 2012.
- [18] B. Tondu, "A closed-form inverse kinematic modelling of a 7R anthropomorphic upper limb based on a joint parametrization," in *Proc. of the IEEE-RAS Int. Conf. on Humanoid Robots (Humanoids)*, 2006, pp. 390–397.
- [19] W. Xiao, *et al.*, "Closed-form inverse kinematics of 6R milling robot with singularity avoidance," *Production Engineering*, vol. 5, no. 1, pp. 103–110, 2011.
- [20] I.-M. Chen and Y. Gao, "Closed-form inverse kinematics solver for reconfigurable robots," in *Proc. of the IEEE Int. Conf. on Robotics and Automation (ICRA)*, 2001, pp. 2395–2400.
- [21] R. C. Luo, T.-W. Lin, and Y.-H. Tsai, "Analytical inverse kinematic solution for modularized 7-DOF redundant manipulators with offsets at shoulder and wrist," in *Proc. of the IEEE/RSJ Int. Conf. on Intelligent Robots and Systems (IROS)*, 2014, pp. 516–521.
- [22] W. Xu, Y. She, and Y. Xu, "Analytical and semi-analytical inverse kinematics of SSRMS-type manipulators with single joint locked failure," *Acta Astronautica*, vol. 105, no. 1, pp. 201–217, 2014.
- [23] I. Zaplana and L. Basanez, "A novel closed-form solution for the inverse kinematics of redundant manipulators through workspace analysis," *Mechanism and Machine Theory*, vol. 121, pp. 829–843, 2018.
- [24] A. J. Elias and J. T. Wen, "Redundancy parameterization and inverse kinematics of 7-DOF revolute manipulators," *Mechanism and Machine Theory*, vol. 204, no. 105824, 2024.
- [25] M. Shimizu, *et al.*, "Analytical inverse kinematic computation for 7-DOF redundant manipulators with joint limits and its application to redundancy resolution," *Transactions on Robotics*, vol. 24, no. 5, pp. 1131–1142, 2008.
- [26] H. Moradi and S. Lee, "Joint limit analysis and elbow movement minimization for redundant manipulators using closed form method," in *Proc. of the Int. Conf. on Intelligent Computing (ICIC)*, 2005, pp. 423–432.
- [27] I. Zaplana, H. Hadfield, and J. Lasenby, "Closed-form solutions for the inverse kinematics of serial robots using conformal geometric algebra," *Mechanism and Machine Theory*, vol. 173, no. 104835, 2022.
- [28] Y. Wei, *et al.*, "General approach for inverse kinematics of nR robots," *Mechanism and Machine Theory*, vol. 75, pp. 97–106, 2014.
- [29] B. E. Paden, "Kinematics and control of robot manipulators," Ph.D. dissertation, EECS Department, University of California, Berkeley, 1986.
- [30] W. Kahan, "Lecture on computational aspects of geometry," University of California, Berkeley, 1983.
- [31] E. Sariyildiz, E. Cakiray, and H. Temeltas, "A comparative study of three inverse kinematic methods of serial industrial robot manipulators in the screw theory framework," *Advanced Robotic Systems*, vol. 8, no. 5, pp. 9–24, 2011.
- [32] P.-F. Lin, M.-B. Huang, and H.-P. Huang, "Analytical solution for inverse kinematics using dual quaternions," *IEEE Access*, vol. 7, pp. 166 190–166 202, 2019.
- [33] T. Yue-sheng and X. Ai-ping, "Extension of the second Paden-Kahan sub-problem and its' application in the inverse kinematics of a manipulator," in *Proc. of the IEEE Conf. on Robotics, Automation and Mechatronics (RAM)*, 2008, pp. 379–381.
- [34] M. Raghaven and B. Roth, "Kinematic analysis of the 6R manipulator of general geometry," in *Proc. of the Int. Symp. on Robotics Research (ISRR)*, 1991, pp. 263–269.
- [35] D. Manocha and J. Canny, "Real time inverse kinematics for general 6R manipulators," in *Proc. of the IEEE Int. Conf. on Robotics and Automation (ICRA)*, vol. 1, 1992, pp. 383–389.
- [36] T. Truong, *et al.*, "General solution for inverse kinematics of six degrees of freedom of a welding robot arm," in *Proc. of the Int. Conf. on System Science and Engineering (ICSSE)*, 2023, pp. 387–394.
- [37] W. Shanda, *et al.*, "Existence conditions and general solutions of closed-form inverse kinematics for revolute serial robots," *Applied Sciences*, vol. 9, no. 20, p. 4365, 2019.
- [38] T. Campos, *et al.*, "Task-based design of ad-hoc modular manipulators," in *Proc. of the IEEE Int. Conf. on Robotics and Automation (ICRA)*, 2019, pp. 6058–6064.
- [39] M. Althoff, *et al.*, "Effortless creation of safe robots from modules through self-programming and self-verification," *Science Robotics*, vol. 4, no. 31, 2019.
- [40] E. Romiti, *et al.*, "An optimization study on modular reconfigurable robots: Finding the task-optimal design," in *IEEE Int. Conf. on Automation Science and Engineering (CASE)*, 2023, pp. 1–8.
- [41] J. K  l, M. Mayer, and M. Althoff, "Timor Python: A toolbox for industrial modular robotics," in *Proc. of the IEEE/RSJ Int. Conf. on Intelligent Robots and Systems (IROS)*, 2023, pp. 424–431.
- [42] K. Leibrandt, L. da Cruz, and C. Bergeles, "Designing robots for reachability and dexterity: Continuum surgical robots as a pretext application," *Transactions on Robotics*, vol. 39, no. 4, pp. 2989–3007, 2023.
- [43] S. B. Liu and M. Althoff, "Optimizing performance in automation through modular robots," in *Proc. of the IEEE Int. Conf. on Robotics and Automation (ICRA)*, 2020, pp. 4044–4050.
- [44] E. M. Hoffman, *et al.*, "Addressing reachability and discrete componentsselection in robotic manipulator design through kineto-static bi-level optimization," *IEEE Robotics and Automation Letters*, vol. 10, no. 3, pp. 2263–2270, 2025.
- [45] R. M. Murray, S. S. Sastry, and L. Zexiang, *A Mathematical Introduction to Robotic Manipulation*, 1st ed. CRC Press, 1994.
- [46] R. Goldman, "Intersection of two lines in three-space," in *Graphics Gems*, A. S. Glassner, Ed., 1994, ch. 3.
- [47] P. Corke and J. Haviland, "Not your grandmother's toolbox—the robotics toolbox reinvented for Python," in *Proc. of the IEEE Int. Conf. on Robotics and Automation (ICRA)*, 2021, pp. 11 357–11 363.
- [48] Y. He and S. Liu, "Analytical inverse kinematics for Franka Emika Panda – a geometrical solver for 7-DOF manipulators with unconventional design," in *Proc. of the IEEE Int. Conf. on Control, Mechatronics and Automation (ICCMA)*, 2021, pp. 194–199.
- [49] J. Haviland and P. Corke, "Manipulator differential kinematics: Part 2: Acceleration and advanced applications," *Robotics & Automation Magazine*, pp. 2–12, 2023.

APPENDIX

We derive additional analytical solutions for specific manipulators that were not denoted in [7] but are solvable using their solutions to the subproblems in Table III. If multiple subproblem decompositions exist for a manipulator, we only present one of them—preferably one where major parts in its derivation can be reused in other manipulator classes. The choice of the basis and end effector is interchangeable by the use of kinematic inversion as per Section IV-C. Hence, each of the following decompositions (e.g., regarding intersecting axes 5 and 6) is representative for problems with the inversed kinematic chain (e.g., intersecting axes 1 and 2).

TABLE III
SUBSET OF THE SUBPROBLEMS PRESENTED BY ELIAS ET AL. [7].

Subproblem	Formulation
SP1	$\min \ \mathbf{R}(\mathbf{h}_i, \theta_i) \mathbf{x}_1 - \mathbf{x}_2\ _2$
SP2	$\min \ \mathbf{R}(\mathbf{h}_i, \theta_i) \mathbf{x}_1 - \mathbf{R}(\mathbf{h}_j, \theta_j) \mathbf{x}_2\ _2$
SP3	$\min \ \ \mathbf{R}(\mathbf{h}_i, \theta_i) \mathbf{x}_1 - \mathbf{x}_2\ _2 - d\ $
SP4	$\min h_i^T \mathbf{R}(\mathbf{h}_j, \theta_j) \mathbf{x}_1 - d $

We denote a vector displacement as $\mathbf{x}_n \in \mathbb{R}^3$, scalars as $d \in \mathbb{R}$, unit vectors of rotation as $\mathbf{h}_n \in \mathbb{R}^3$ and corresponding angles as θ_n . The given formulations are independent of any particular manipulator kinematics.

The desired orientation ${}^0\mathbf{R}_{EE}$, and the static rotation between the last joint and the end effector ${}^6\mathbf{R}_{EE}$ are known. ${}^0\mathbf{R}_6$ is known via (11) and defines the joint rotations via (12):

$${}^0\mathbf{R}_6 = {}^0\mathbf{R}_{EE} {}^6\mathbf{R}_{EE}^T \quad (11)$$

$$\stackrel{(2)}{=} {}^0\mathbf{R}_1 {}^1\mathbf{R}_2 {}^2\mathbf{R}_3 {}^3\mathbf{R}_4 {}^4\mathbf{R}_5 {}^5\mathbf{R}_6. \quad (12)$$

Without loss of generality, we define our base frame Σ_0 such that ${}^0\mathbf{p}_1 = \mathbf{0}$. Consequentially, the position kinematics in (1) can be rewritten as:

$$\begin{aligned} {}^1\mathbf{p}_6 &= {}^0\mathbf{p}_{EE} - {}^0\mathbf{p}_1 - {}^0\mathbf{R}_6 {}^6\mathbf{p}_{EE} \\ &= {}^0\mathbf{R}_1 {}^1\mathbf{p}_2 + {}^0\mathbf{R}_2 {}^2\mathbf{p}_3 + {}^0\mathbf{R}_3 {}^3\mathbf{p}_4 \\ &\quad + {}^0\mathbf{R}_4 {}^4\mathbf{p}_5 + {}^0\mathbf{R}_5 {}^5\mathbf{p}_6. \end{aligned} \quad (13)$$

We simplify either (13) or (12) and apply one of the subproblems introduced in Table III (denoted by “SP(1...4)”) to obtain analytical solutions for a subset of the joint angles. We repeat the process of reformulation and subproblem-application until the solutions to all joint angles are known. We denote rotations with known joint angles by ${}^{j-1}\mathbf{R}_j^*$.

a) Spherical Wrist Manipulators: Let the last three axes of a manipulator intersect in a common point such that ${}^4\mathbf{p}_5$ and ${}^5\mathbf{p}_6$ are zero, so that (13) becomes

$${}^1\mathbf{p}_6 = {}^0\mathbf{R}_1 ({}^1\mathbf{p}_2 + {}^1\mathbf{R}_2 ({}^2\mathbf{p}_3 + {}^2\mathbf{R}_3 {}^3\mathbf{p}_4)). \quad (14)$$

This decouples the orientation IK with joint angles $(\theta_4, \theta_5, \theta_6)$ from the position IK with joint angles $(\theta_1, \theta_2, \theta_3)$. We obtain $\theta_4, \theta_5, \theta_6$, and hence ${}^3\mathbf{R}_4^*, {}^4\mathbf{R}_5^*, {}^5\mathbf{R}_6^*$ following the derivations in [7, Section 4.1], where the authors also propose solutions to $\theta_1, \theta_2, \theta_3$ for manipulators of class 9.

If the second and third axes intersect, ${}^2\mathbf{p}_3$ can be set to zero by kinematic remodeling. As the manipulator has a spherical wrist, we know that ${}^4\mathbf{p}_5 = {}^5\mathbf{p}_6 = \mathbf{0}$. We can rewrite (14) and leverage the norm-preserving property of rotations to obtain:

$${}^1\mathbf{p}_6 = {}^0\mathbf{R}_1 ({}^1\mathbf{p}_2 + {}^1\mathbf{R}_2 ({}^2\mathbf{R}_3 {}^3\mathbf{p}_4)) \quad (15)$$

$$\Leftrightarrow {}^0\mathbf{R}_1^T {}^1\mathbf{p}_6 - {}^1\mathbf{p}_2 = {}^1\mathbf{R}_2 {}^2\mathbf{R}_3 {}^3\mathbf{p}_4 \quad (16)$$

$$\Rightarrow 0 = \|\|{}^0\mathbf{R}_1^T {}^1\mathbf{p}_6 - {}^1\mathbf{p}_2\|_2 - \|\|{}^3\mathbf{p}_4\|_2. \quad (17)$$

The solutions we obtain for θ_1 via SP3 from (17) pose a superset to the solutions for θ_1 in (16). The extraneous solutions that arise from such simplifications, e.g., by norm-preservation, can always be found and excluded after inserting them into the original equation once we obtain the remaining joint angles (in this case, θ_2 and θ_3). Reformulating (16)

and inserting θ_1 yields (18), from which we obtain θ_2, θ_3 by applying SP2.

$$0 = \|\|{}^1\mathbf{R}_2^T ({}^0\mathbf{R}_1^{*T} {}^1\mathbf{p}_6 - {}^1\mathbf{p}_2) - {}^2\mathbf{R}_3 {}^3\mathbf{p}_4\|_2 \quad (18)$$

If the first and second axis are parallel, we can choose $\mathbf{h}_1 = \mathbf{h}_2$. A unit vector is invariant to rotations about itself. This results in the following identities, shown by the example of a rotation about the parallel axes $\mathbf{h}_1, \mathbf{h}_2$:

$${}^0\mathbf{R}_2 \mathbf{h}_1 = {}^0\mathbf{R}_1 {}^1\mathbf{R}_2 \mathbf{h}_1 = {}^0\mathbf{R}_1 \mathbf{h}_1 = \mathbf{h}_1 \quad (19)$$

$$\mathbf{h}_1^T {}^0\mathbf{R}_2 = \mathbf{h}_1^T {}^0\mathbf{R}_1 {}^1\mathbf{R}_2 = \mathbf{h}_1^T {}^1\mathbf{R}_2 = \mathbf{h}_1^T. \quad (20)$$

Hence, multiplying (14) by \mathbf{h}_1 or \mathbf{h}_2 simplifies it to:

$$0 = \mathbf{h}_1^T {}^2\mathbf{R}_3 {}^3\mathbf{p}_4 - \mathbf{h}_1^T ({}^1\mathbf{p}_6 - {}^1\mathbf{p}_2 - {}^2\mathbf{p}_3). \quad (21)$$

We solve (21) for θ_3 by using SP4 and arrive at (22) after rephrasing and employing the L2 norm to (14). Applying SP3 to (22) yields θ_1 .

$$0 = \|\|{}^0\mathbf{R}_1^T {}^1\mathbf{p}_6 - {}^1\mathbf{p}_2\|_2 - \|\|{}^2\mathbf{R}_3 {}^3\mathbf{p}_4 + {}^2\mathbf{p}_3\|_2 \quad (22)$$

Rewriting (14) yields (23), to which we apply SP1 for θ_2 :

$$0 = {}^1\mathbf{R}_2 ({}^2\mathbf{p}_3 + {}^2\mathbf{R}_3 {}^3\mathbf{p}_4) - ({}^0\mathbf{R}_1^{*T} {}^1\mathbf{p}_6 - {}^1\mathbf{p}_2). \quad (23)$$

b) Three Parallel Axes: In [7], decompositions for this kinematic class are derived when the second, third, and fourth axes are parallel. We extend this by proposing:

When the first three axes are parallel and axes five and six intersect, $\mathbf{h}_1 = \mathbf{h}_2 = \mathbf{h}_3$. We can choose ${}^5\mathbf{p}_6 = \mathbf{0}$ and rewrite (13) as (24). Multiplying (24) by \mathbf{h}_1 yields (25).

$${}^1\mathbf{p}_6 = {}^0\mathbf{R}_1 {}^1\mathbf{p}_2 + {}^0\mathbf{R}_2 {}^2\mathbf{p}_3 + {}^0\mathbf{R}_3 {}^3\mathbf{p}_4 + {}^0\mathbf{R}_3 {}^3\mathbf{R}_4 {}^4\mathbf{p}_5 \quad (24)$$

$$0 = \mathbf{h}_1^T {}^3\mathbf{R}_4 {}^4\mathbf{p}_5 - \mathbf{h}_1^T ({}^1\mathbf{p}_6 - {}^1\mathbf{p}_2 - {}^2\mathbf{p}_3 - {}^3\mathbf{p}_4) \quad (25)$$

We use SP4 on (25) to obtain θ_4 . Multiplication of (12) by \mathbf{h}_5 and \mathbf{h}_1 leads to (26), to which we apply SP4 for θ_6 . Finally, we combine the rotations about the first three axes in a common formulation of SP4 in (27) for $\theta_{03} = \theta_1 + \theta_2 + \theta_3$:

$$0 = \mathbf{h}_5^T {}^5\mathbf{R}_6 {}^6\mathbf{R}_6^T \mathbf{h}_1 - \mathbf{h}_5^T {}^3\mathbf{R}_4 {}^4\mathbf{p}_5 \quad (26)$$

$$0 = \mathbf{h}_4^T {}^0\mathbf{R}_3 {}^3\mathbf{R}_3^T {}^6\mathbf{R}_6 {}^5\mathbf{R}_6^T \mathbf{h}_5 - \mathbf{h}_4^T \mathbf{h}_5. \quad (27)$$

We define a unit vector $\mathbf{h}_n \in \mathbb{R}^3$ that is normal to \mathbf{h}_5 , as well as the auxiliary variable $\delta \in \mathbb{R}^3$:

$$\delta = {}^3\mathbf{p}_4 + {}^3\mathbf{R}_4 {}^4\mathbf{p}_5. \quad (28)$$

Multiplying (12) with \mathbf{h}_n yields (29), from which we obtain θ_5 via SP1. We use L2 norm-preservation on (13) to arrive at (30), on which we use SP3 for θ_2 :

$$0 = {}^4\mathbf{R}_5 {}^5\mathbf{R}_6^* \mathbf{h}_n - {}^3\mathbf{R}_4^T {}^0\mathbf{R}_3 {}^3\mathbf{p}_4 \mathbf{h}_n \quad (29)$$

$$0 = \|\|{}^1\mathbf{R}_2 {}^2\mathbf{p}_3 + {}^1\mathbf{p}_2\|_2 - \|\|{}^1\mathbf{p}_6 - {}^0\mathbf{R}_3^* \delta\|_2. \quad (30)$$

Using norm-preservation on (13) yields (31), to which we apply SP1 for θ_1 . We multiply (12) by the vector normal to $\mathbf{h}_3, \mathbf{h}'_n$, to arrive at (32). Applying SP1 to (32) yields θ_3 .

$$0 = \|\|{}^0\mathbf{R}_1 ({}^1\mathbf{p}_2 + {}^1\mathbf{R}_2 {}^2\mathbf{p}_3) + {}^0\mathbf{R}_3^* \delta - {}^1\mathbf{p}_6\|_2 \quad (31)$$

$$0 = {}^2\mathbf{R}_3^T \mathbf{h}'_n - {}^0\mathbf{R}_3^T {}^0\mathbf{R}_1^* {}^1\mathbf{R}_2^* \mathbf{h}'_n. \quad (32)$$

Automatic Geometric Decomposition for Analytical Inverse Kinematics: Derivations on 1R, 2R, 3R, 4R, and 5R Manipulators

Daniel Ostermeier¹, Jonathan K  lz^{1,2}, and Matthias Althoff^{1,2}

TABLE I
SUBSET OF THE SUBPROBLEMS PRESENTED BY ELIAS ET AL. [1].

Subproblem	Formulation
SP1	$\min \ \mathbf{R}(\mathbf{h}_i, \theta_i)\mathbf{x}_1 - \mathbf{x}_2\ _2$
SP2	$\min \ \mathbf{R}(\mathbf{h}_i, \theta_i)\mathbf{x}_1 - \mathbf{R}(\mathbf{h}_j, \theta_j)\mathbf{x}_2\ _2$
SP3	$\min \ \ \mathbf{R}(\mathbf{h}_i, \theta_i)\mathbf{x}_1 - \mathbf{x}_2\ _2 - d\ $
SP4	$\min \mathbf{h}_i^T \mathbf{R}(\mathbf{h}_j, \theta_j)\mathbf{x}_1 - d $
SP5	$\mathbf{x}_0 + \mathbf{R}(\mathbf{h}_i, \theta_i)\mathbf{x}_1 = \mathbf{R}(\mathbf{h}_j, \theta_j)(\mathbf{x}_2 + \mathbf{R}(\mathbf{h}_k, \theta_k)\mathbf{x}_3)$
SP6	$\mathbf{h}_i^T \mathbf{R}(\mathbf{h}_j, \theta_j)\mathbf{x}_1 + \mathbf{h}_l^T \mathbf{R}(\mathbf{h}_k, \theta_k)\mathbf{x}_2 = d_1$
	$\mathbf{h}_m^T \mathbf{R}(\mathbf{h}_j, \theta_j)\mathbf{x}_3 + \mathbf{h}_n^T \mathbf{R}(\mathbf{h}_k, \theta_k)\mathbf{x}_4 = d_2$

We denote a vector displacement as $\mathbf{x}_n \in \mathbb{R}^3$, scalars as $d_n \in \mathbb{R}$, unit vectors of rotation as $\mathbf{h}_n \in \mathbb{R}^3$ and corresponding angles as θ_n . The given formulations are independent of any particular manipulator kinematics.

I. EXTENDED APPENDIX: AN OVERVIEW

Manipulators with fewer than four joint axes can be parametrized using only position or orientation constraints. For manipulators with four or more joints, we use a full 6DOF pose for our input constraints. As this parametrization can impose more constraints than needed for 4R and 5R manipulators, it is up to the user to ensure the given rotation and position are compatible for the respective manipulator. Unreachable poses result in least-squares solution sets. As we perform the inverse kinematic calculations for some angles based on orientation constraints and some based on position constraints, some solutions will be viable to achieve *either* the desired position or orientation, but not both. Hence, we compute the forward kinematics based on the obtained solution set and rule out (denote as approximate) solutions that do not result in the desired pose.

In the following derivations, we only consider cases of intersecting/parallel axes that resemble an analytically solvable manipulator, i.e., one that is not redundant in any pose with respect to the chosen parametrization (position/orientation IK). All proposed cases are hereby strictly necessary to check for, as additional intersecting/parallel axes can lead to solution continuities within the subproblems if not considered.

All analytically solvable manipulators with four (or fewer) rotational axes are solvable by the proposed subproblem decompositions (sometimes only after kinematic inversion). Contrarily, 5R manipulators must meet at least one of the following sufficient criteria to be analytically solvable:

- The last or first two axes 1,2 (5,6) intersect.
- The intermediate axes 2,3 (3,4) intersect while the axes 3,4 (2,3) are parallel.
- Any three consecutive axes are parallel.

Additional intersecting/parallel axes – as long as they do not lead to implicit redundancies – lead to further simplifications, which we also account for.

II. 1R MANIPULATORS

The forward kinematics for a 1R manipulator are given via:

$${}^0\mathbf{p}_{EE} = {}^0\mathbf{p}_1 + {}^0\mathbf{R}_1 {}^1\mathbf{p}_{EE} \quad (1)$$

$${}^0\mathbf{R}_{EE}^* = {}^0\mathbf{R}_1 {}^1\mathbf{R}_{EE}^* \quad (2)$$

The IK can be solved either given a desired position by applying SP1 to (3) or via a desired orientation by applying SP1 to (4).

$$\|{}^0\mathbf{R}_1 {}^1\mathbf{p}_{EE} - ({}^0\mathbf{p}_{EE} - {}^0\mathbf{p}_1)\| = 0 \quad (3)$$

$$\|{}^0\mathbf{R}_1 \mathbf{h}_n - {}^0\mathbf{R}_{EE}^* {}^1\mathbf{R}_{EE}^{*T} \mathbf{h}_n\| = 0 \quad (4)$$

III. 2R MANIPULATORS

The forward kinematics for a 2R manipulator are given via:

$${}^0\mathbf{p}_{EE} = {}^0\mathbf{p}_1 + {}^0\mathbf{R}_1 ({}^1\mathbf{p}_2 + {}^1\mathbf{R}_2 {}^2\mathbf{p}_2) \quad (5)$$

$${}^0\mathbf{R}_2^* = {}^0\mathbf{R}_{EE}^* {}^2\mathbf{R}_{EE}^{*T} = {}^0\mathbf{R}_1 {}^1\mathbf{R}_2 \quad (6)$$

a) *Position IK*: Two cases must be distinguished when solving the IK for a given position: the axes intersect, or they do not. If the two axes of the manipulator intersect, we can choose ${}^1\mathbf{p}_2 = 0$ to obtain (7) from (5). We subsequently use SP2 on (7) to obtain θ_1, θ_2 .

$${}^0\mathbf{R}_1^T ({}^0\mathbf{p}_{EE} - {}^0\mathbf{p}_1) - {}^1\mathbf{R}_2 {}^2\mathbf{p}_{EE} = 0 \quad (7)$$

If, on the other hand, the two axes do not intersect, we leverage norm-preservation on (5) to obtain (8). We apply SP3 to (8) to obtain θ_2 .

$$\|{}^1\mathbf{R}_2 {}^2\mathbf{p}_{EE} + {}^1\mathbf{p}_2\| - \|{}^1\mathbf{p}_{EE}\| = 0 \quad (8)$$

By reformulating (5) and inserting the calculated θ_2 , we obtain (9). We obtain θ_1 by applying SP1 to (9).

$${}^0\mathbf{R}_1 ({}^1\mathbf{p}_2 + {}^1\mathbf{R}_2^* {}^2\mathbf{p}_{EE}) - ({}^0\mathbf{p}_{EE} - {}^0\mathbf{p}_1) = 0 \quad (9)$$

¹Department of Computer Engineering, Technical University of Munich, 85748 Garching, Germany. {daniel.sebastian.ostermeier, jonathan.kuelz, althoff}@tum.de

²Munich Center for Machine Learning (MCML)

b) Orientation IK: The orientation kinematics can only be analytically solved if the two axes are not parallel. Otherwise, the manipulator is redundant in every configuration for its orientation IK. We obtain a vector \mathbf{h}_n that is normal to the rotated axis \mathbf{h}_1 and the axis \mathbf{h}_2 via (10). After reformulating (6) and right-multiply with \mathbf{h}_n , we obtain (11). Applying SP2 to (11) subsequently yields θ_1, θ_2 .

$$\mathbf{h}_n = {}^0\mathbf{R}_{EE}^{*T} \mathbf{h}_1 \times \mathbf{h}_2 \quad (10)$$

$${}^0\mathbf{R}_1^T {}^0\mathbf{R}_2^* \mathbf{h}_n - {}^1\mathbf{R}_2 \mathbf{h}_n = 0 \quad (11)$$

IV. 3R MANIPULATORS

The forward kinematics for a 3R manipulator are given via (12). In the following, we will use ${}^1\mathbf{p}_{EE}$ for conciseness as denoted in (13).

$${}^0\mathbf{p}_{EE} = {}^0\mathbf{p}_1 + {}^0\mathbf{R}_1 {}^1\mathbf{p}_2 + {}^0\mathbf{R}_2 {}^2\mathbf{p}_3 + {}^0\mathbf{R}_3 {}^3\mathbf{p}_{EE} \quad (12)$$

$${}^1\mathbf{p}_{EE} = {}^0\mathbf{p}_{EE} - {}^0\mathbf{p}_1 \quad (13)$$

$${}^0\mathbf{R}_3 = {}^0\mathbf{R}_{EE} {}^3\mathbf{R}_{EE}^{*T} = {}^0\mathbf{R}_1 {}^1\mathbf{R}_2 {}^2\mathbf{R}_3 \quad (14)$$

a) Position IK: If no two consecutive axes are parallel and no axes intersect, we can directly apply SP5 to (12) and obtain $\theta_1, \theta_2, \theta_3$.

If the first two axes intersect we can choose ${}^1\mathbf{p}_2 = 0$, rephrase (12) according to (15), and then leverage norm-preservation to obtain (16). Applying SP3 to (16) yields θ_3 .

$${}^1\mathbf{R}_2^T {}^0\mathbf{R}_1^T {}^1\mathbf{p}_{EE} = {}^2\mathbf{R}_3 {}^3\mathbf{p}_{EE} + {}^2\mathbf{p}_3 \quad (15)$$

$$\|{}^1\mathbf{p}_{EE}\| = \|{}^2\mathbf{R}_3 {}^3\mathbf{p}_{EE} + {}^2\mathbf{p}_3\| \quad (16)$$

Inserting the calculated value for θ_3 into a rephrased version of (12) yields (17). Applying SP2 to (17) yields θ_1, θ_2 .

$${}^0\mathbf{R}_1^T {}^1\mathbf{p}_{EE} = {}^1\mathbf{R}_2 ({}^2\mathbf{p}_3 + {}^2\mathbf{R}_3 {}^3\mathbf{p}_{EE}) \quad (17)$$

If the first two axes are parallel we can choose $\mathbf{h}_1 = \mathbf{h}_2$. We left-multiply (12) with \mathbf{h}_1 to obtain (18). Applying SP4 to (18) yields θ_3 . By inserting θ_3 into a rephrased version of (12), we get (19), which simplifies to (20) after leveraging the norm-preserving property.

$$\mathbf{h}_1^T ({}^1\mathbf{p}_{EE} - {}^1\mathbf{p}_2 - {}^2\mathbf{p}_3) = \mathbf{h}_1^T {}^2\mathbf{R}_3 {}^3\mathbf{p}_4 \quad (18)$$

$${}^0\mathbf{R}_1^T {}^1\mathbf{p}_{EE} = {}^1\mathbf{R}_2 ({}^2\mathbf{p}_3 + {}^2\mathbf{R}_3 {}^3\mathbf{p}_{EE}) + {}^1\mathbf{p}_2 \quad (19)$$

$$\|{}^1\mathbf{p}_{EE}\| = \|{}^1\mathbf{R}_2 ({}^2\mathbf{p}_3 + {}^2\mathbf{R}_3 {}^3\mathbf{p}_{EE}) + {}^1\mathbf{p}_2\| \quad (20)$$

We apply SP3 to (20) to obtain θ_2 . Plugging θ_2, θ_3 into (12) yields (21), from which we obtain θ_1 via SP1.

$${}^0\mathbf{R}_1^T {}^1\mathbf{p}_{EE} - {}^1\mathbf{R}_2^* ({}^2\mathbf{p}_3 + {}^2\mathbf{R}_3 {}^3\mathbf{p}_{EE}) = 0 \quad (21)$$

b) Orientation IK: If no consecutive two axes are parallel we rephrase (14), left-multiply with \mathbf{h}_3^T and right-multiply with \mathbf{h}_1 to obtain (22), which simplifies to (23). Applying SP4 to (23) yields θ_2 .

$$\mathbf{h}_3^T {}^0\mathbf{R}_3^{*T} {}^0\mathbf{R}_1 \mathbf{h}_1 = \mathbf{h}_3^T {}^2\mathbf{R}_3 {}^1\mathbf{R}_2^T \mathbf{h}_1 \quad (22)$$

$$\mathbf{h}_3^T {}^0\mathbf{R}_3^{*T} \mathbf{h}_1 = \mathbf{h}_3^T {}^1\mathbf{R}_2^T \mathbf{h}_1 \quad (23)$$

We insert θ_2 into a rephrased version of (14) and right-multiply with \mathbf{h}_3 . This yields (24), which simplifies to (25). We obtain θ_1 from (25) by applying SP1.

$${}^0\mathbf{R}_1^T {}^0\mathbf{R}_3^{*2} \mathbf{R}_3^T \mathbf{h}_3 = {}^1\mathbf{R}_2^* \mathbf{h}_3 \quad (24)$$

$${}^0\mathbf{R}_1^T {}^0\mathbf{R}_3^* \mathbf{h}_3 = {}^1\mathbf{R}_2^* \mathbf{h}_3 \quad (25)$$

Let \mathbf{h}_n denote a vector normal to \mathbf{h}_3 . We again rephrase (14), insert θ_1, θ_2 , and right-multiply with \mathbf{h}_n to obtain (26). Applying SP1 to (26) finally yields θ_3 .

$${}^2\mathbf{R}_3 \mathbf{h}_n = {}^1\mathbf{R}_2^{*T} {}^0\mathbf{R}_1^{*T} {}^0\mathbf{R}_3^* \mathbf{h}_n \quad (26)$$

If the first two axes are parallel We rephrase according to (22), but without left-multiplication with \mathbf{h}_3^T , which, after simplification, yields (27). Applying SP1 to (27) yields θ_3 .

$${}^0\mathbf{R}_3^{*T} \mathbf{h}_1 = {}^2\mathbf{R}_3^T \mathbf{h}_1 \quad (27)$$

Inserting θ_3 into a rephrased version of (14) yields (28), which simplifies to (29). We obtain θ_1 by applying SP1 to (29).

$${}^0\mathbf{R}_1^T {}^0\mathbf{R}_3^{*2} \mathbf{R}_3^T \mathbf{h}_2 = {}^1\mathbf{R}_2 \mathbf{h}_2 \quad (28)$$

$${}^0\mathbf{R}_1^T {}^0\mathbf{R}_3^{*2} \mathbf{R}_3^T \mathbf{h}_2 = \mathbf{h}_2 \quad (29)$$

$${}^1\mathbf{R}_2 \mathbf{h}_3 = {}^0\mathbf{R}_1^{*T} {}^0\mathbf{R}_3^{*2} \mathbf{R}_3^T \mathbf{h}_3 \quad (30)$$

Inserting θ_1, θ_3 into a rephrased version of (14) yields (30). We apply SP1 to (30) for θ_2 .

If the manipulator does not match any of the above cases, we use kinematic inversion and solve the inverted kinematic chain with the previous derivations.

V. 4R MANIPULATORS

In contrast to the prior manipulators with less than four degrees of freedom, we now consider both the end effector position and orientation as given.

The forward position kinematics for a 4R manipulator are given by (31). As the rotation ${}^0\mathbf{R}_4^*$ is known as per the orientation kinematics in (33), we can break down (31) to the translation ${}^1\mathbf{p}_4$ according to (32).

$${}^0\mathbf{p}_{EE} = {}^0\mathbf{p}_1 + {}^0\mathbf{R}_1 {}^1\mathbf{p}_2 + {}^0\mathbf{R}_2 {}^2\mathbf{p}_3 + {}^0\mathbf{R}_3 {}^3\mathbf{p}_4 + {}^0\mathbf{R}_4 {}^4\mathbf{p}_{EE} \quad (31)$$

$${}^1\mathbf{p}_4 = {}^0\mathbf{p}_{EE} - {}^0\mathbf{p}_1 - {}^0\mathbf{R}_4 {}^4\mathbf{p}_{EE} = {}^0\mathbf{R}_1 {}^1\mathbf{p}_2 + {}^0\mathbf{R}_2 {}^2\mathbf{p}_3 + {}^0\mathbf{R}_3 {}^3\mathbf{p}_4 \quad (32)$$

$${}^0\mathbf{R}_4^* = {}^0\mathbf{R}_{EE}^* {}^4\mathbf{R}_{EE}^{*T} = {}^0\mathbf{R}_1 {}^1\mathbf{R}_2 {}^2\mathbf{R}_3 {}^3\mathbf{R}_4 \quad (33)$$

If no consecutive pair of axes is parallel or intersects, we can rewrite (32) according to (34), to which we directly apply SP5 to obtain $\theta_1, \theta_2, \theta_3$.

$${}^0\mathbf{R}_1^T {}^1\mathbf{p}_4 - {}^1\mathbf{p}_2 = {}^1\mathbf{R}_2 ({}^2\mathbf{p}_3 + {}^2\mathbf{R}_3 {}^3\mathbf{p}_4) \quad (34)$$

$${}^3\mathbf{R}_4 \mathbf{h}_n - {}^2\mathbf{R}_3^{*T} {}^1\mathbf{R}_2^{*T} {}^0\mathbf{R}_1^{*T} {}^0\mathbf{R}_4^* \mathbf{h}_n = 0 \quad (35)$$

Further, we insert the obtained joint values into (33) and, after rephrasing, obtain (35). The vector \mathbf{h}_n is hereby chosen normal to \mathbf{h}_4 . We obtain θ_4 by applying SP1 to (35).

If the first two axes are parallel, we can choose $\mathbf{h}_1 = \mathbf{h}_2$. We left-multiply (32) with \mathbf{h}_1^T to obtain (36), from which we obtain θ_3 via SP4.

$$\mathbf{h}_1^T {}^2\mathbf{R}_3 {}^3\mathbf{p}_4 = \mathbf{h}_1^T ({}^1\mathbf{p}_4 - {}^1\mathbf{p}_2 - {}^2\mathbf{p}_3) \quad (36)$$

Rephrasing (32) and inserting θ_3 yields (37), which, via norm-preservation, results in (38). Applying SP3 to (38) yields θ_1 .

$${}^0\mathbf{R}_1^T {}^1\mathbf{p}_4 - {}^1\mathbf{p}_2 = {}^1\mathbf{R}_2 ({}^2\mathbf{p}_3 + {}^2\mathbf{R}_3^* {}^3\mathbf{p}_4) \quad (37)$$

$$\|{}^0\mathbf{R}_1^T {}^1\mathbf{p}_4 - {}^1\mathbf{p}_2\| = \|{}^2\mathbf{p}_3 + {}^2\mathbf{R}_3^* {}^3\mathbf{p}_4\| \quad (38)$$

Inserting θ_1 back into (37) yields (39), from which we obtain θ_2 via SP1. Finally, we insert $\theta_1, \theta_2, \theta_3$ into (33) and right-multiply by the vector \mathbf{h}_n – which we choose such that it is normal to \mathbf{h}_4 – to obtain (40). We retrieve θ_4 by applying SP1 to (40).

$${}^1\mathbf{R}_2 ({}^2\mathbf{p}_3 + {}^2\mathbf{R}_3^* {}^3\mathbf{p}_4) - ({}^0\mathbf{R}_1^{*T} {}^1\mathbf{p}_4 - {}^1\mathbf{p}_2) = 0 \quad (39)$$

$${}^3\mathbf{R}_4^T \mathbf{h}_n - {}^0\mathbf{R}_4^{*T} {}^0\mathbf{R}_1^* {}^1\mathbf{R}_2^* {}^2\mathbf{R}_3^* \mathbf{h}_n = 0 \quad (40)$$

If the second and third axis are parallel, we can choose $\mathbf{h}_2 = \mathbf{h}_3$. We start off by rephrasing (32) according to (41). When left-multiplying (41) with \mathbf{h}_1 , it simplifies to (42), to which we apply SP4 to obtain θ_1 .

$${}^2\mathbf{R}_3^T {}^1\mathbf{R}_2^T {}^0\mathbf{R}_1^T {}^1\mathbf{p}_4 = {}^2\mathbf{R}_3^T ({}^1\mathbf{R}_2^T {}^1\mathbf{p}_2 + {}^2\mathbf{p}_3) + {}^3\mathbf{p}_4 \quad (41)$$

$$\mathbf{h}_2^T {}^0\mathbf{R}_1^T {}^1\mathbf{p}_4 = \mathbf{h}_2^T ({}^1\mathbf{p}_2 + {}^2\mathbf{p}_3 + {}^3\mathbf{p}_4) \quad (42)$$

We rephrase (32) according to (34), insert θ_1 , and leverage norm-preservation to obtain (43). Applying SP3 to (43) yields θ_3 . Inserting θ_1, θ_3 back into (34) yields (44), which we can solve via SP1 for θ_2 .

$$\|{}^0\mathbf{R}_1^{*T} {}^1\mathbf{p}_4 - {}^1\mathbf{p}_2\| = \|{}^2\mathbf{R}_3 {}^3\mathbf{p}_4 + {}^2\mathbf{p}_3\| \quad (43)$$

$${}^1\mathbf{R}_2 ({}^2\mathbf{p}_3 + {}^2\mathbf{R}_3^* {}^3\mathbf{p}_4) - ({}^0\mathbf{R}_1^{*T} {}^1\mathbf{p}_4 - {}^1\mathbf{p}_2) = 0 \quad (44)$$

Just like before, we insert $\theta_1, \theta_2, \theta_3$ into (33) and right-multiply by the vector \mathbf{h}_n (normal to \mathbf{h}_4) to obtain (40). We retrieve θ_4 by applying SP1 to (40).

If the second and third axis intersect, we can choose ${}^2\mathbf{p}_3 = 0$, which simplifies (32) to (45). Employing norm-preservation on (45) results in (46), from which we obtain θ_1 through SP3.

$${}^1\mathbf{p}_4 - {}^0\mathbf{R}_1 {}^1\mathbf{p}_2 = {}^0\mathbf{R}_1 {}^1\mathbf{R}_2 {}^2\mathbf{R}_3 {}^3\mathbf{p}_4 \quad (45)$$

$$\|{}^1\mathbf{p}_4 - {}^0\mathbf{R}_1 {}^1\mathbf{p}_2\| = \|{}^3\mathbf{p}_4\| \quad (46)$$

Rephrasing (45) and inserting θ_1 yields (47), to which we apply SP2 to obtain θ_2, θ_3 .

$${}^1\mathbf{R}_2^T ({}^0\mathbf{R}_1^{*T} {}^1\mathbf{p}_4 - {}^1\mathbf{p}_2) = {}^2\mathbf{R}_3 {}^3\mathbf{p}_4 \quad (47)$$

Just as in the two prior cases, we insert $\theta_1, \theta_2, \theta_3$ into (33) and right-multiply by the vector \mathbf{h}_n (normal to \mathbf{h}_4) to obtain (40). We then retrieve θ_4 by applying SP1 to (40).

If the third and fourth axis intersect, we can choose ${}^3\mathbf{p}_4 = 0$ and hence simplify (32) to (48), which can be

rephrased to (49). Imposing the L2 norm on both sides of (49) results in (50), from which we obtain θ_1 via SP3.

$${}^1\mathbf{p}_4 = {}^0\mathbf{R}_1 {}^1\mathbf{p}_2 + {}^0\mathbf{R}_2 {}^2\mathbf{p}_3 \quad (48)$$

$${}^0\mathbf{R}_1^T {}^1\mathbf{p}_4 - {}^1\mathbf{p}_2 = {}^1\mathbf{R}_2 {}^2\mathbf{p}_3 \quad (49)$$

$$\|{}^0\mathbf{R}_1^T {}^1\mathbf{p}_4 - {}^1\mathbf{p}_2\| = \|{}^2\mathbf{p}_3\| \quad (50)$$

After inserting θ_1 back into (49), we can directly apply SP1 to retrieve θ_2 . Finally, we rephrase (33), insert θ_1, θ_2 , and right-multiply with a vector \mathbf{h}_n that is normal to \mathbf{h}_4 to obtain (51). Applying SP2 to (51) then yields θ_3, θ_4 .

$${}^2\mathbf{R}_3^T {}^1\mathbf{R}_2^{*T} {}^0\mathbf{R}_1^{*T} {}^0\mathbf{R}_4^* \mathbf{h}_n = {}^3\mathbf{R}_4 \mathbf{h}_n \quad (51)$$

If the first and last two axes intersect in a separate point, we can choose ${}^1\mathbf{p}_2 = 0$ and ${}^3\mathbf{p}_4 = 0$ to simplify (32) to (52). We rephrase (52) according to (53), to which we apply SP2 to obtain θ_1, θ_2 .

$${}^1\mathbf{p}_4 = {}^0\mathbf{R}_2 {}^2\mathbf{p}_3 \quad (52)$$

$${}^0\mathbf{R}_1^T {}^1\mathbf{p}_4 = {}^1\mathbf{R}_2 {}^2\mathbf{p}_3 \quad (53)$$

We rephrase (33), insert θ_1, θ_2 , and right-multiply by a vector \mathbf{h}_n that is normal to \mathbf{h}_4 to obtain (54). Applying SP2 to (54) subsequently yields θ_3, θ_4 .

$${}^2\mathbf{R}_3^T {}^1\mathbf{R}_2^{*T} {}^0\mathbf{R}_1^{*T} {}^0\mathbf{R}_4^* \mathbf{h}_n = {}^3\mathbf{R}_4 \mathbf{h}_n \quad (54)$$

If the last three axes intersect in a common point (i.e., form a spherical wrist), we can choose ${}^2\mathbf{p}_3 = 0$ and ${}^3\mathbf{p}_4 = 0$ to simplify (32) to (55). We directly obtain θ_1 from (55) by applying SP1.

$${}^1\mathbf{p}_4 = {}^0\mathbf{R}_1 {}^1\mathbf{p}_2 \quad (55)$$

Rephrasing (33) and inserting θ_1 yields (56). Right-multiplying (56) with \mathbf{h}_4 simplifies it to (56). Applying SP2 to (56) yields θ_2, θ_3 .

$${}^1\mathbf{R}_2^T {}^0\mathbf{R}_1^{*T} {}^0\mathbf{R}_4^* = {}^2\mathbf{R}_3 {}^3\mathbf{R}_4 \quad (56)$$

$${}^1\mathbf{R}_2^T {}^0\mathbf{R}_1^{*T} {}^0\mathbf{R}_4^* \mathbf{h}_4 = {}^2\mathbf{R}_3 \mathbf{h}_4 \quad (57)$$

Again, we insert $\theta_1, \theta_2, \theta_3$ into (33) and right-multiply by the vector \mathbf{h}_n (normal to \mathbf{h}_4) to obtain (40). We then retrieve θ_4 by applying SP1 to (40).

In any case, we use kinematic inversion and check if the inverted kinematic chain matches a case that is more specialized (i.e., represents a case that employs *simpler* subproblems) than that of the non-inverted one. We hereby first check for a spherical wrist (i.e., three axes at either end of the manipulator intersecting in a common point) and then all the other cases. The most general case (no consecutive intersecting or parallel axes) is only chosen if, and only if, no other case matches.

VI. 5R MANIPULATORS

As mentioned Section I, only certain 5R manipulators are currently known to us to be analytically solvable per our method. Hence, the following list of cases is not exhaustive. Non-redundant (analytically solvable) 5R manipulators might exist that fall into neither of the following categories.

Like for 4R manipulators, we consider both the desired end effector position and orientation as given. When leveraging the same simplifications as in (32), we obtain a concise formulation for the forward kinematics of a 5R manipulator via (58) and (59).

$${}^1p_5 = {}^0R_1 {}^1p_2 + {}^0R_2 {}^2p_3 + {}^0R_3 {}^3p_4 + {}^0R_4 {}^4p_5 \quad (58)$$

$${}^0R_5^* = {}^0R_{EE}^* {}^5R_{EE}^{*T} = {}^0R_1 {}^1R_2 {}^2R_3 {}^3R_4 {}^4R_5 \quad (59)$$

If the last two axes intersect, we can choose ${}^4p_5 = 0$ such that (58) simplifies to (60). We obtain $\theta_1, \theta_2, \theta_3$ by applying SP5 to (60). We rephrase (59), insert $\theta_1, \theta_2, \theta_3$, and right-multiply with a vector h_n that is normal to h_5 to obtain (61). Applying SP2 to (61) yields θ_4, θ_5 .

$${}^0R_1^T {}^1p_5 = {}^1p_2 + {}^1R_2 {}^2p_3 + {}^1R_2 {}^2R_3 {}^3p_4 \quad (60)$$

$${}^3R_4^T {}^2R_3^* {}^1R_2^* {}^0R_1^* {}^0R_5^* h_n = {}^4R_5 h_n \quad (61)$$

If the last two axes intersect while also the second and third axis intersect, we can choose ${}^4p_5 = 0$ and ${}^2p_3 = 0$ such that (58) simplifies to (62). Using the norm-preservation property, we further simplify (62) to (63). We apply SP3 to (63) to obtain θ_1 .

$${}^0R_1^T {}^1p_5 - {}^1p_2 = {}^1R_2 {}^2R_3 {}^3p_4 \quad (62)$$

$$\|{}^0R_1^T {}^1p_5 - {}^1p_2\| = \|{}^3p_4\| \quad (63)$$

Inserting θ_1 into a rephrased version of (62) yields (64), to which we apply SP2 to retrieve θ_2, θ_3 .

$${}^1R_2^T ({}^0R_1^{*T} {}^1p_5 - {}^1p_2) = {}^2R_3 {}^3p_4 \quad (64)$$

Finally, we insert $\theta_1, \theta_2, \theta_3$ into (59), rephrase it, and right-multiply with a vector h_n that is normal to h_5 to obtain (65). We then apply SP2 to (65) to obtain θ_4, θ_5 .

$${}^4R_5 h_n = {}^3R_4^T {}^2R_3^* {}^1R_2^* {}^0R_1^* {}^0R_5^* h_n \quad (65)$$

If the last two axes intersect while also the first two axes intersect, we can choose ${}^4p_5 = 0$ and ${}^1p_2 = 0$ such that (58) simplifies to (66). Using norm-preservation on (66) yields (67), to which we apply SP3 for θ_3 .

$${}^0R_1^T {}^1p_5 = {}^1R_2 ({}^2p_3 + {}^2R_3 {}^3p_4) \quad (66)$$

$$\|{}^1p_5\| = \|{}^2p_3 + {}^2R_3 {}^3p_4\| \quad (67)$$

After inserting θ_3 back into (66), we can directly apply SP2 to it and subsequently obtain θ_1, θ_2 . For θ_4, θ_5 , we follow the same procedure as in the previous case to end up at (65), to which we then obtain SP2 to yield θ_4, θ_5 .

If the last two axes intersect while the first two axes are parallel, we can choose ${}^4p_5 = 0$ and $h_1 = h_2$. Equation (58) then simplifies to (60). Left-multiplication of (60)

by h_1^T further simplifies it to (68). We apply SP4 to (68) to obtain θ_3 .

$$h_1^T {}^2R_3 {}^3p_4 = h_1^T ({}^1p_5 - {}^1p_2 - {}^2p_3) \quad (68)$$

Inserting θ_3 into (60) yields (69), which, after using norm-preservation, simplifies to (70). Applying SP3 to (70) yields θ_1 . We insert θ_1 back into (69), apply SP1 to it, and thus obtain θ_2 .

$${}^0R_1^T {}^1p_5 - {}^1p_2 = {}^1R_2 ({}^2p_3 + {}^2R_3 {}^3p_4) \quad (69)$$

$$\|{}^0R_1^T {}^1p_5 - {}^1p_2\| = \|{}^2p_3 + {}^2R_3 {}^3p_4\| \quad (70)$$

For θ_4, θ_5 , we follow the same procedure as in the previous two case.

If the last two axes intersect while the second and third axis are parallel, we can choose ${}^4p_5 = 0$ and $h_2 = h_3$. Equation (58) then simplifies to (60). Left-multiplication of (60) by h_2^T further simplifies it to (71). Applying SP4 to (71) yields θ_1 .

$$h_2^T {}^0R_1^T {}^1p_5 = h_2^T ({}^1p_2 + {}^2p_3 + {}^3p_4) \quad (71)$$

We rephrase (60) and insert θ_1 , such that we obtain (72). Leveraging norm-preservation, (72) further simplifies to (73). We apply SP3 to (73) to retrieve θ_3 .

$${}^2R_3 {}^3p_4 + {}^2p_3 = {}^1R_2^T ({}^0R_1^{*T} {}^1p_5 - {}^1p_2) \quad (72)$$

$$\|{}^2R_3 {}^3p_4 + {}^2p_3\| = \|{}^0R_1^{*T} {}^1p_5 - {}^1p_2\| \quad (73)$$

We obtain $\theta_2, \theta_4, \theta_5$ by following the same procedure as in the previous case.

If the second and third axis are parallel while the third and fourth axis intersect, we can choose ${}^3p_4 = 0$ and $h_2 = h_3$. This simplifies (58) to (74). Left-multiplication of (74) by h_2^T further simplifies it to (75).

$${}^0R_1^T {}^1p_5 = {}^1p_2 + {}^1R_2 ({}^2p_3 + {}^2R_3 {}^3R_4 {}^4p_5) \quad (74)$$

$$h_2^T {}^0R_1^T {}^1p_5 - h_2^T {}^3R_4 {}^4p_5 = h_2^T ({}^1p_2 + {}^2p_3) \quad (75)$$

Further, we rephrase (59) as (76). Left-multiplication by h_2^T and right-multiply by h_5 simplifies (76) to (77). The two equations (75) and (77) now resemble a system of equations that we can solve for θ_1, θ_4 through SP6.

$${}^1R_2^T {}^0R_1^T {}^0R_5^* {}^4R_5^T - {}^2R_3 {}^3R_4 = 0 \quad (76)$$

$$h_2^T {}^0R_1^T {}^0R_5^* h_5 - h_2^T {}^3R_4 h_5 = 0 \quad (77)$$

We rephrase (58) as (78) and insert θ_1, θ_4 . Leveraging norm-preservation (78) simplifies to (79). Applying SP3 to (79) yields θ_3 .

$${}^1R_2^T ({}^0R_1^{*T} {}^1p_5 - {}^1p_2) = {}^2R_3 {}^3R_4 {}^4p_5 + {}^2p_3 \quad (78)$$

$$\|{}^0R_1^{*T} {}^1p_5 - {}^1p_2\| = \|{}^2R_3 {}^3R_4 {}^4p_5 + {}^2p_3\| \quad (79)$$

Inserting $\theta_1, \theta_3, \theta_4$ back into (74) results in (80), from which we obtain θ_2 via SP1.

$${}^0R_1^{*T} {}^1p_5 - {}^1p_2 = {}^1R_2 ({}^2p_3 + {}^2R_3 {}^3R_4 {}^4p_5) \quad (80)$$

Finally, we rephrase (59) and insert $\theta_1, \theta_2, \theta_3, \theta_4$ to obtain (81), where \mathbf{h}_n represents a normal vector to \mathbf{h}_5 . Applying SP1 to (81) then yields θ_5 .

$${}^4\mathbf{R}_5\mathbf{h}_n = {}^3\mathbf{R}_4^{*T} {}^2\mathbf{R}_3^{*T} {}^1\mathbf{R}_2^{*T} {}^0\mathbf{R}_1^{*T} {}^0\mathbf{R}_5^*\mathbf{h}_n \quad (81)$$

If the second and third axis are parallel while the third and fourth axis intersect, and the fourth and fifth axis are parallel, we can choose ${}^3\mathbf{p}_4 = 0$, $\mathbf{h}_2 = \mathbf{h}_3$, and $\mathbf{h}_4 = \mathbf{h}_5$. This simplifies (58) to (74). We rephrase (59) as (82). Left- and right-multiplication of (82) with \mathbf{h}_2^T and \mathbf{h}_5 simplifies the equation to (83). Applying SP4 to (83) yields θ_1 .

$${}^0\mathbf{R}_1^T {}^0\mathbf{R}_5^* = {}^1\mathbf{R}_2 {}^2\mathbf{R}_3 {}^3\mathbf{R}_4 {}^4\mathbf{R}_5 \quad (82)$$

$$\mathbf{h}_1^T {}^0\mathbf{R}_1^T {}^0\mathbf{R}_5^*\mathbf{h}_5 = \mathbf{h}_1^T\mathbf{h}_5 \quad (83)$$

We insert θ_1 into (74), and, after left-multiplication with \mathbf{h}_2^T , obtain (84). Applying SP4 to (84) yields θ_4 .

$$\mathbf{h}_2^T {}^3\mathbf{R}_4 {}^4\mathbf{p}_5 = \mathbf{h}_2^T ({}^0\mathbf{R}_1^{*T} {}^1\mathbf{p}_5 - {}^1\mathbf{p}_2 - {}^2\mathbf{p}_3) \quad (84)$$

We obtain $\theta_3, \theta_4, \theta_5$ by following the same procedure as in the previous case where the fourth and fifth axis were not parallel.

If the first three axes are parallel, we can choose $\mathbf{h}_1 = \mathbf{h}_2 = \mathbf{h}_3$. We rephrase (59) according to (85). Right-multiplication of (85) by \mathbf{h}_1 results in (86), to which we apply SP2 to obtain θ_4, θ_5 .

$${}^4\mathbf{R}_5 {}^0\mathbf{R}_5^{*T} = {}^3\mathbf{R}_4^T {}^2\mathbf{R}_3^T {}^1\mathbf{R}_2^T {}^0\mathbf{R}_1^T \quad (85)$$

$${}^4\mathbf{R}_5 {}^0\mathbf{R}_5^{*T}\mathbf{h}_1 = {}^3\mathbf{R}_4^T\mathbf{h}_1 \quad (86)$$

As the first three axes are parallel, such that $\mathbf{h}_1 = \mathbf{h}_2 = \mathbf{h}_3$, their induced rotation can be described by a single rotation ${}^0\mathbf{R}_3$ about one of the equivalent axes. The rotation angle hereby consists of the sum of all three rotations, i.e., $\theta_{1,2,3} = \theta_1 + \theta_2 + \theta_3$. Using this definition, inserting θ_4, θ_5 into (59), and rephrasing it yields (87). We apply SP1 to (87) to obtain $\theta_{1,2,3}$.

$${}^0\mathbf{R}_3\mathbf{h}_n = {}^0\mathbf{R}_5^* {}^4\mathbf{R}_5^{*T} {}^3\mathbf{R}_4^{*T}\mathbf{h}_n \quad (87)$$

Inserting the obtained values for θ_4, θ_5 and $\theta_{1,2,3}$ into (58) yields, after rephrasing, (88). Leveraging norm-preservation (88) simplifies to (89). We apply SP1 to (89) to obtain θ_2 . After inserting θ_2 back into (88), we can directly apply SP1 to obtain θ_1 .

$${}^1\mathbf{p}_5 - {}^0\mathbf{R}_3^* ({}^3\mathbf{p}_4 + {}^3\mathbf{R}_4^* {}^4\mathbf{p}_5) = {}^0\mathbf{R}_1 ({}^1\mathbf{p}_2 + {}^1\mathbf{R}_2 {}^2\mathbf{p}_3) \quad (88)$$

$$\|{}^1\mathbf{p}_5 - {}^0\mathbf{R}_3^* ({}^3\mathbf{p}_4 + {}^3\mathbf{R}_4^* {}^4\mathbf{p}_5)\| = \|{}^1\mathbf{p}_2 + {}^1\mathbf{R}_2 {}^2\mathbf{p}_3\| \quad (89)$$

Finally, we use the definition of ${}^0\mathbf{R}_3^* = {}^0\mathbf{R}_1 {}^1\mathbf{R}_2 {}^2\mathbf{R}_3$, insert θ_1, θ_2 , and right-multiply by \mathbf{h}_n – a normal vector to \mathbf{h}_3 – to obtain (90). We obtain θ_3 by applying SP1 to (90).

$${}^2\mathbf{R}_3\mathbf{h}_n = {}^1\mathbf{R}_2^{*T} {}^0\mathbf{R}_1^{*T} {}^0\mathbf{R}_3^*\mathbf{h}_n \quad (90)$$

If the first three axes are parallel to each other, while the last two axes are also parallel, we can choose

$\mathbf{h}_1 = \mathbf{h}_2 = \mathbf{h}_3$ and $\mathbf{h}_4 = \mathbf{h}_5$. First, we left-multiply (58) by \mathbf{h}_1^T to obtain (91). We then apply SP4 to (91) to obtain θ_4 .

$$\mathbf{h}_1^T {}^3\mathbf{R}_4 {}^4\mathbf{p}_5 = \mathbf{h}_1^T ({}^1\mathbf{p}_5 - {}^1\mathbf{p}_2 - {}^2\mathbf{p}_3 - {}^3\mathbf{p}_4) \quad (91)$$

We insert θ_4 into (59), rephrase according to (92), and right-multiply with \mathbf{h}_1 to obtain (93). Applying SP1 to (93) then yields θ_5 .

$${}^4\mathbf{R}_5 {}^0\mathbf{R}_5^{*T} = {}^3\mathbf{R}_4^{*T} {}^2\mathbf{R}_3^T {}^1\mathbf{R}_2^T {}^0\mathbf{R}_1^T \quad (92)$$

$${}^4\mathbf{R}_5 {}^0\mathbf{R}_5^{*T}\mathbf{h}_1 = {}^3\mathbf{R}_4^{*T}\mathbf{h}_1 \quad (93)$$

Starting from (87), we then follow the same procedure as proposed in the last case – where $\mathbf{h}_4 \neq \mathbf{h}_5$ – to obtain $\theta_1, \theta_2, \theta_3$.

If the second, third, and fourth axis are parallel, we can choose $\mathbf{h}_2 = \mathbf{h}_3 = \mathbf{h}_4$. We rephrase (58) as done in (89) and left-multiply with \mathbf{h}_2^T to obtain (94). Applying SP4 to (94) yields θ_1 .

$$\mathbf{h}_2^T {}^0\mathbf{R}_1^T {}^1\mathbf{p}_5 = \mathbf{h}_2^T ({}^1\mathbf{p}_2 + {}^2\mathbf{p}_3 + {}^3\mathbf{p}_4 + {}^4\mathbf{p}_5) \quad (94)$$

Rephrasing (59) and inserting θ_1 yields (95), which, after right-multiplication with \mathbf{h}_2 simplifies to (96). We apply SP1 to (96) to obtain θ_5 .

$${}^4\mathbf{R}_5 {}^0\mathbf{R}_5^{*T} {}^0\mathbf{R}_1^* = {}^3\mathbf{R}_4^T {}^2\mathbf{R}_3^T {}^1\mathbf{R}_2^T \quad (95)$$

$${}^4\mathbf{R}_5 {}^0\mathbf{R}_5^{*T} {}^0\mathbf{R}_1^*\mathbf{h}_2 = \mathbf{h}_2 \quad (96)$$

Just like in (87), we can represent ${}^1\mathbf{R}_4 = {}^1\mathbf{R}_2 {}^2\mathbf{R}_3 {}^3\mathbf{R}_4$ via a single rotation about one of the three parallel axes (e.g., \mathbf{h}_2) by a single angle $\theta_{2,3,4} = \theta_2 + \theta_3 + \theta_4$. To obtain $\theta_{2,3,4}$, we insert θ_1, θ_5 into (59), which yields (97), where \mathbf{h}_n is a vector normal to the parallel axes. Applying SP1 to (97) yields $\theta_{2,3,4}$.

$${}^1\mathbf{R}_4\mathbf{h}_n = {}^0\mathbf{R}_1^{*T} {}^0\mathbf{R}_5^* {}^4\mathbf{R}_5^{*T}\mathbf{h}_n \quad (97)$$

We left-multiply (58) by ${}^0\mathbf{R}_4^T = {}^1\mathbf{R}_4^{*T} {}^1\mathbf{R}_0^{*T}$ and rephrase it such that we obtain (98). Using norm-preservation on (98) yields (99). Applying SP3 to (99) yields θ_3 . We insert θ_3 back into (98) and then directly apply SP1 to obtain θ_4 .

$${}^1\mathbf{R}_4^{*T} ({}^0\mathbf{R}_1^{*T} {}^1\mathbf{p}_5 - {}^1\mathbf{p}_2) - {}^4\mathbf{p}_5 = {}^3\mathbf{R}_4^T ({}^2\mathbf{R}_3^T {}^2\mathbf{p}_3 + {}^3\mathbf{p}_4) \quad (98)$$

$$\|{}^1\mathbf{R}_4^{*T} ({}^0\mathbf{R}_1^{*T} {}^1\mathbf{p}_5 - {}^1\mathbf{p}_2) - {}^4\mathbf{p}_5\| = \|{}^2\mathbf{R}_3^T {}^2\mathbf{p}_3 + {}^3\mathbf{p}_4\| \quad (99)$$

Inserting θ_3, θ_4 into the definition of ${}^1\mathbf{R}_4$ yields (100), where \mathbf{h}_n represent a normal vector to the three parallel axes. Applying SP1 to (100) finally yields θ_2 .

$${}^1\mathbf{R}_2\mathbf{h}_n = {}^1\mathbf{R}_4^* {}^3\mathbf{R}_4^{*T} {}^2\mathbf{R}_3^T\mathbf{h}_n \quad (100)$$

If the last three axes intersect in a common point (i.e., form a spherical wrist), we can choose ${}^3\mathbf{p}_4 = {}^4\mathbf{p}_5 = 0$, which simplifies (58) to (101). Leveraging norm-preservation, we further obtain (102), to which we apply

SP3 to retrieve θ_1 . We then insert θ_1 back into (101) and subsequently use SP1 to obtain θ_2 .

$${}^0R_1^T {}^1p_5 - {}^1p_2 = {}^1R_2 {}^2p_3 \quad (101)$$

$$\|{}^0R_1^T {}^1p_5 - {}^1p_2\| = \|{}^1R_2 {}^2p_3\| \quad (102)$$

We rephrase (59) as (103). Right-multiplication with h_5 simplifies (103) to (104), to which we apply SP2 to obtain θ_3, θ_4

$${}^2R_3^T {}^1R_2^T {}^0R_1^T R_5^* = {}^3R_4 {}^4R_5 \quad (103)$$

$${}^2R_3^T {}^1R_2^T {}^0R_1^T R_5^* h_5 = {}^3R_4 h_5 \quad (104)$$

We obtain θ_5 by following the same steps as for (81), where we insert $\theta_1, \theta_2, \theta_3, \theta_4$ into (59), right multiply with a normal vector to h_5 , and apply SP1.

If the last three axes intersect to form a spherical wrist, while the first two axes intersect in a point separate to that of the wrist, we can choose ${}^1p_2 = 0$ in addition to ${}^3p_4 = {}^4p_5 = 0$, which simplifies (101) to (105). We apply SP2 to (105) to obtain θ_1, θ_2 .

$${}^0R_1^T {}^1p_5 = {}^1R_2 {}^2p_3 \quad (105)$$

For $\theta_3, \theta_4, \theta_5$ we follow the same procedure as in the previous case where the first two axes are non-intersecting.

In any case, we use kinematic inversion and check if the inverted kinematic chain matches a case that is more specialized (i.e., represents a case that employs *simpler* subproblems) than that of the non-inverted one. We hereby first check for three parallel axes, then for two intersecting axes at either end of the manipulator and then all the others. E.g., if the first three axes of a manipulator are parallel and the last two axes intersect, we assign the manipulator to the kinematic family of three initial parallel axes. If, even after kinematic inversion, the manipulator does not match any of the proposed cases, it is to our current knowledge not solvable via our method.

REFERENCES

- [1] A. J. Elias and J. T. Wen, “IK-Geo: Unified robot inverse kinematics using subproblem decomposition,” *Mechanism and Machine Theory*, vol. 209, no. 105971, 2025.